Available online at www.sciencedirect.com
ScienceDirect
Journal of Sound and Vibration 297 (2006) 1000–1024
JOURNAL OF SOUND AND VIBRATION
www.elsevier.com/locate/jsvi

Reliability analysis of randomly vibrating structures with parameter uncertainties

Sayan Gupta[a], C.S. Manohar[b,*]

[a]Department of Civil Engineering, Technical University of Delft, Stevinweg 1, PO Box 5048, 2600 GA, Delft, The Netherlands
[b]Department of Civil Engineering, Indian Institute of Science, Bangalore 560012, India

Received 2 August 2005; received in revised form 2 May 2006; accepted 5 May 2006
Available online 3 July 2006

Abstract

The problem of reliability analysis of randomly driven, stochastically parametered, vibrating structures is considered. The excitation components are assumed to be jointly stationary, Gaussian random processes. The randomness in structural parameters is modelled through a vector of mutually correlated, non-Gaussian random variables. The structure is defined to be safe if a set of response quantities remain within prescribed thresholds over a given duration of time. An approximation for the failure probability, conditioned on structure randomness, is first formulated in terms of recently developed multivariate extreme value distributions. An estimate of the unconditional failure probability is subsequently obtained using a method based on Taylor series expansion. This has involved the evaluation of gradients of the multivariate extreme value distribution, conditioned on structure random variables, with respect to the basic variables. Analytical and numerical techniques for computing these gradients have been discussed. Issues related to the accuracy of the proposed method have been examined. The proposed method has applications in reliability analysis of vibrating structural series systems, where different failure modes are mutually dependent. Illustrative examples presented include the seismic fragility analysis of a piping network in a nuclear power plant.

1. Introduction

The problem of reliability analysis of randomly parametered vibrating systems is of central importance in the safety assessment of structures, under environmental loads, such as earthquakes, wind or ocean waves. The limit state functions for discrete multi-degree vibrating systems can, in general, be represented as $g_i[\mathbf{X}, \mathbf{Y}(t), \mathbf{\Lambda}, t] = 0$, $(i = 1, \ldots, n)$. Here, $\mathbf{X}$ is the vector of random variables that model physical or aleatory uncertainties, $\mathbf{\Lambda}$ is the vector of random variables that represent modelling or epistemic uncertainties, $\mathbf{Y}(t)$ is the vector of random processes that represent time-varying load effects on the structure and t denotes time. The performance functions, in general, are nonlinear functions of their arguments and components of $\mathbf{X}$ and $\mathbf{\Lambda}$ which are, in general, mutually dependent and non-Gaussian in nature [1]. The probability of failure, P_{f_i}, with

*Corresponding author: Tel.: +91 80 2293 3121; fax: +91 80 2360 0404.
E-mail addresses: S.Gupta@tudelft.nl (S. Gupta), manohar@civil.iisc.ernet.in (C.S. Manohar).

0022-460X/$ - see front matter © 2006 Elsevier Ltd. All rights reserved.
doi:10.1016/j.jsv.2006.05.010

respect to the ith performance function $g_i(\cdot)$, is given by

$$P_{f_i} = 1 - P[g_i\{\mathbf{X}, \mathbf{Y}(t), \mathbf{\Lambda}, t\} > 0 \ \forall t \in (t_0, t_0 + T)], \tag{1}$$

where, $g_i(\cdot) > 0$ denotes safe configuration, T is the time duration of interest and t_0 is initial time. For the structural system considered as a whole, the definition of structural failure requires attention to configuration of the failure modes, $i = 1, \ldots, n$. The simplest of these configurations is perhaps the series system, in which, the system failure is given by

$$P_f = 1 - P\left[\bigcap_{i=1}^{n}\{g_i(\mathbf{X}, \mathbf{Y}(t), \mathbf{\Lambda}, t) > 0 \ \forall t \in (t_0, t_0 + T)\}\right]. \tag{2}$$

The treatment of more general configuration of failure modes is more complicated. The difficulties, here, are due to the time-varying nature of the performance functions, identification of important failure modes, treatment of mutual dependencies between failure modes and modelling of load effect redistribution upon violation of individual failure modes. In the present study, we restrict our attention to evaluation of P_f, as given by Eq. (2), with reference to reliability of randomly excited, stochastically parametered, dynamical systems.

2. Background literature

Defining the performance function of vibrating structures in terms of extreme values of the structure response processes, enables treatment of such time-varying reliability problems (as in Eq. (2)) in a time-invariant format [2,3]. One of the commonly used approaches is to study the first passage failures based on the assumption that the number of times a specified level is crossed can be modelled as a Poisson counting process. The application of this theory leads to the well-known Rice's formula [4] for estimating the mean out-crossing rate and requires the joint probability density functions (pdf) of the constituent response processes and their instantaneous time derivatives. This knowledge is, however, presently available only for a limited class of problems. For Gaussian random processes, these assumptions lead to exponential models for the first passage times and Gumbel models for the extremes over a specified duration. Results based on this assumption and further refinements are available in literature [5–7]. For scalar non-Gaussian processes, linearization schemes have been applied to determine bounds on their exceedance probabilities [8–10]. Approximate estimates of the mean outcrossing rates of translation non-Gaussian processes have been obtained by studying the outcrossing characteristics of corresponding Gaussian processes, obtained from Nataf's transformations [11,12]. Several studies on extreme value distributions for non-Gaussian processes, obtained as quadratic transformations of Gaussian processes, such as the Von Mises stress process, are available in the literature. Geometric approaches based on transforming the problem into the polar coordinate space have been used for developing analytical expressions for the mean outcrossing rate of Von Mises stress in Gaussian excited linear structures [13] and for constructing the pdf of the Von Mises stress in plates and shells [14]. Studies on second-order stochastic Volterra series have been carried out and expressions for their outcrossing rates have been derived in terms of the joint characteristic function of the process and its instantaneous time derivative [15–17]. The use of the maximum entropy method in constructing the joint pdf for the Von Mises stress and its instantaneous time derivative, in linear structures under Gaussian excitations, has been explored recently [18]. Computational algorithms, such as the response surface method, has also been used to study the extremes of Von Mises stress in nonlinear structures under Gaussian excitations [19].

Outcrossing rates of vector random processes have been studied in the context of problems in load combinations [20] and in structural reliability [21–25]. The focus of many of these studies has been in determining the exceedance probability of the sum of component processes, and the outcrossing event has been formulated as a scalar process outcrossing. Some of these results have been used in the geometric approach considered by Leira [26,27] in the studies on development of multivariate extreme value distributions for vector Gaussian/non-Gaussian random processes. In some recent studies, approximations have been developed for multivariate extreme value distributions for vectors of Gaussian processes [28,29] and non-Gaussian processes obtained as nonlinear transformations of vector Gaussian processes [30]. The crux of these approximations are based on the principle that multipoint random processes can be used to model the level crossing statistics of vector Gaussian/non-Gaussian processes.

These studies, however, do not take into account the effect of structure randomness and modelling uncertainties that invariably exist in real-life engineering structures [31,32]. Studies on the importance of considering the effect of structure randomness in reliability analysis of highly reliable structures under random dynamic loads, has been reported in the literature [33–35]. Chreng and Wen [36] estimated the probability of first excursion across specified barriers of randomly parametered, nonlinear vibrating trusses, by employing an equivalent linearization scheme in conjunction with a second-order reliability method. Zhang and Der Kiureghian [37] studied first passage failure probabilities of random structures under deterministic excitations. The limit surfaces of these structures were found to be highly nonlinear and consisted of multiple design points. These authors used first-order reliability method and concepts of series system reliability, to obtain bounds for the first excursion probabilities. Brenner and Bucher [38] used stochastic finite-element method to discretize structure property random fields in nonlinear multi-degree of freedom systems. They, first, fitted a response surface in the space spanned by a subset of structure random variables which were found to have significant effect on the structure reliability. Subsequently, an adaptive importance sampling was carried out to estimate first passage failure probabilities. Mahadevan and Mehta [39] discussed matrix condensation techniques for stochastic finite-element methods, for reliability analyses of stochastically parametered frame structures. The present authors, in an earlier study [40], obtained estimates of first passage failure probabilities of stochastically parametered skeletal structures under random excitations. The structure property random fields, assumed to be non-Gaussian, were discretized using the optimal linear expansion scheme. Extreme value theory was used to obtain the first passage probabilities, conditioned on the structure random variables. The unconditional failure probabilities were computed by carrying out adaptive importance sampling in the space spanned by the vector of non-Gaussian random variables, representing structural uncertainties.

The present study focusses on the evaluation of reliability of randomly parametered structural systems, subjected to stationary, vector Gaussian random excitations. The uncertainties in the problem are grouped into the following three categories:

(a) *Dynamic loads*: These are modelled as a vector of stationary, Gaussian random processes,
(b) *Structural capacities* (*such as permissible stresses*): These are modelled, in general, as a vector of mutually dependent, non-Gaussian random variables $\mathbf{Z}^*$, and
(c) Structural properties that influence the structural matrices, such as, the elastic constants, mass density and damping properties: these are, again, modelled as a vector of mutually dependent, non-Gaussian random variables $\mathbf{X}$.

The study assumes that the influence of uncertainties in loads and structural capacities, $\mathbf{Z}^*$, on structural reliability is much stronger than the influence of $\mathbf{X}$. Accordingly, we first determine the structural failure probability, conditioned on $\mathbf{X}$, by using results from theory of extremes of vector Gaussian/non-Gaussian random processes. The associated unconditional failure probability is subsequently approximated by developing a Taylor series expansion for the conditional failure probability, in the $\mathbf{X}$-space. The study discusses computational and analytical procedures for implementing the procedure. A set of illustrative examples are presented where the response quantities of interest constitute vectors of Gaussian/non-Gaussian processes. The accuracy of the theoretical predictions are examined using limited Monte Carlo simulations. Subsequently, the applicability of the method is illustrated in the context of seismic fragility analysis of a piping network in a nuclear power plant.

3. Problem statement

3.1. Conditional extreme value distribution

A structure under random dynamic loads is considered. The governing equations of motion, when discretized using finite elements and expressed in a general form, is given by

$$\mathbf{M}\ddot{\mathbf{Y}}(t) + \mathbf{C}\dot{\mathbf{Y}}(t) + \mathbf{K}\mathbf{Y}(t) = \mathbf{F}(t). \tag{3}$$

Here, $\mathbf{M}$, $\mathbf{C}$ and $\mathbf{K}$ are, respectively, the mass, damping and stiffness matrices; $\ddot{\mathbf{Y}}, \dot{\mathbf{Y}}$ and $\mathbf{Y}$ are, respectively, the unknown vectors of nodal acceleration, velocity and displacements and $\mathbf{F}(t)$ denotes a vector of jointly stationary, zero-mean, Gaussian random forces. If geometric and/or material nonlinear behavior of the structure is considered, $\mathbf{K}$ is a nonlinear function of $\mathbf{Y}(t)$ and $\dot{\mathbf{Y}}(t)$. Let $\mathbf{X}$ be the vector of random variables representing the uncertainties in the elastic, mass and damping properties. These random variables are, in general, non-Gaussian and mutually dependent. The structural matrices $\mathbf{M}$, $\mathbf{C}$ and $\mathbf{K}$ are, thus, functions of $\mathbf{X}$. In case of earthquake base motions, the specification of $\mathbf{F}(t)$, also, becomes dependent on $\mathbf{X}$. Response quantities of interest, such as displacements, stress resultants, stress components or reactions, are denoted by a n-dimensional vector of random processes, $\mathbf{Z}(t)$, which are, in general, expressed as

$$\begin{aligned}\mathbf{Z}(t) &= \hat{Q}[\ddot{\mathbf{Y}}(t,\mathbf{X}), \dot{\mathbf{Y}}(t,\mathbf{X}), \mathbf{Y}(t,\mathbf{X}), \mathbf{X}, t] \\ &= Q[\mathbf{F}(t), \mathbf{M}(\mathbf{X}), \mathbf{C}(\mathbf{X}), \mathbf{K}(\mathbf{X}), \mathbf{X}, t].\end{aligned} \tag{4}$$

Depending on the problem, $Q[\cdot]$ could be linear or nonlinear and could be explicitly dependent on $\mathbf{X}$. In this study, we assume that structural failure occurs if one or more components of $\mathbf{Z}(t)$, exceeds the corresponding permissible thresholds, Z_i^*, $(i = 1, \ldots, n)$, during the time interval $(t_0, t_0 + T)$. These permissible thresholds, are also modelled as a vector of random variables, which are, in general, taken to be mutually dependent and non-Gaussian. We define the performance function $g_i = Z_i^* - Z_i(t, \mathbf{X})$, $(i = 1, \ldots, n)$, and consider that these associated failure modes are in series. This would mean that we deem the structure to have failed if any one of the associated limit states are violated. Consequently, the structural failure is given by

$$P_f = 1 - P\left[\bigcap_{i=1}^{n} Z_i(t,\mathbf{X}) \leqslant Z_i^* \ \forall t \in (t_0, t_0 + T)\right]. \tag{5}$$

Here, $P[\cdot]$ denotes probability measure and $Z_i(t, \mathbf{X})$ and Z_i^*, respectively, denote the ith component of the n-dimensional vectors $\mathbf{Z}(t, \mathbf{X})$ and $\mathbf{Z}^*$. Note that for stationary random processes, $t_0 \to \infty$. The evaluation of this probability constitutes a problem in time variant reliability analysis. Introducing the random variable $Z_{i_m} = \max_{t_0 \leqslant t \leqslant t_0+T} Z_i(t, \mathbf{X})$ and noting that $P_f = 1 - P[\bigcap_{i=1}^{n} Z_{i_m} \leqslant Z_i^*]$, the problem can be formulated in a time invariant format. The response vector conditioned on $\mathbf{X}$, $\mathbf{Z}(t|\mathbf{X})$, is a vector of mutually correlated, random processes. We define $N_i(Z_i^*, t_0, t_0 + T)$ to be the number of times level Z_i^* is crossed in the interval $(t_0, t_0 + T)$ for each $Z_i(t|\mathbf{X})$. For sufficiently high thresholds Z_i^*, the crossings may be assumed to be rare with zero memory. We assume that $\mathbf{N} = \{N_i(Z_i^*, t_0, t_0 + T)\}_{i=1}^{n}$ constitutes a vector of mutually correlated Poisson random variables [28]. The correlation between the components of $\mathbf{N}$ can be expressed explicitly by introducing a transformation, whereby $\mathbf{N}$ is expressed in terms of a vector of a set of mutually independent Poisson random variables [41,42]. If $n(n+1)/2$ mutually independent, Poisson random variables, with parameters $\{\lambda_i\}_{i=1}^{n(n+1)/2}$, are introduced for n-dimensional vector $\mathbf{N}$, the multivariate extreme value distribution is shown [28] to be given by

$$P_{Z_{m_1} \ldots Z_{m_n}|\mathbf{X}}(Z_1^*, \ldots, Z_n^*|\mathbf{X}) = \exp\left[-\sum_{i=1}^{n(n+1)/2} \lambda_i\right]. \tag{6}$$

Expressions for determining the parameters $\{\lambda_i\}_{i=1}^{n(n+1)/2}$, which, in turn, depend on the covariance matrix of $\mathbf{Z}(t|\mathbf{X})$, have been recently developed for vector Gaussian processes [28] and for vector non-Gaussian processes obtained as nonlinear transformations of Gaussian processes [30]. For vector Gaussian processes, it has also been shown that the marginal distribution $P_{Z_{m_i}|\mathbf{X}}(Z_i^*|\mathbf{X})$ for Z_{m_i} obtained from Eq. (6) follows a Gumbel model, given by

$$P_{Z_{m_i}|\mathbf{X}}(Z_i^*|\mathbf{X}) = \exp\left[-\frac{T}{2\pi}\frac{\gamma_{2_i}}{\gamma_{0_i}}\exp\left\{-\frac{1}{2}\left(\frac{Z_i^* - \mu_i}{\gamma_{0_i}}\right)^2\right\}\right], \tag{7}$$

which conforms to the existing models in the literature for extreme value distributions of scalar, Gaussian random processes. Here, γ_{2_i} and γ_{0_i} are the spectral moments given by $\gamma_{j_i} = [\int_{-\infty}^{\infty} \omega^j S_{ii}(\omega|\mathbf{X})\,\mathrm{d}\omega]^{0.5}$, $(j = 0, 2)$,

ω is the frequency, μ_i is the mean of the process $Z_i(t|\mathbf{X})$, with $S_{ii}(\omega|\mathbf{X})$ being its corresponding power spectral density (PSD) function, conditioned on $\mathbf{X}$.

3.2. Unconditional failure probability

Introducing the notation $\Psi(\mathbf{X})$ to represent the multivariate/univariate extreme value distribution, conditioned on $\mathbf{X}$, the unconditional failure probability is given by

$$P_f = 1 - \int_{-\infty}^{\infty} \Psi(\mathbf{X}) p_{\mathbf{X}}(\mathbf{x})\, d\mathbf{x} = 1 - \langle \Psi(\mathbf{X}) \rangle_{\mathbf{X}}. \tag{8}$$

Here, $p_{\mathbf{X}}(\cdot)$ is the joint pdf of $\mathbf{X}$ and $\langle\cdot\rangle_{\mathbf{X}}$ represents the mathematical expectation with respect to $\mathbf{X}$. For the sake of simplicity, we omit writing the subscript $\mathbf{X}$ in the remaining part of the paper. The problem of evaluation of P_f, thus, reduces to the problem of finding $\langle \Psi(\mathbf{X}) \rangle$. For a m-dimensional vector $\mathbf{X}$, the evaluation of $\langle \Psi(\mathbf{X}) \rangle$ requires a m-dimensional integration. However, since the functional dependence of $\Psi(\mathbf{X})$ on $\mathbf{X}$ would, in most real-life situations, be available only implicitly through structural analysis codes, closed form solutions for $\langle \Psi(\mathbf{X}) \rangle$ is seldom possible. Traditional methods of numerical integration of Eq. (8) could require, depending on the step size, a large number of $\Psi(\mathbf{X})$ evaluations. In most situations, evaluation of $\Psi(\mathbf{X})$ is through a complex code. This would make numerical integrations computationally intensive. On the other hand, an approximation for $\langle \Psi(\mathbf{X}) \rangle$ can be obtained by expanding $\langle \Psi(\mathbf{X}) \rangle$ in a Taylor series, around the mean vector $\mathbf{X_0}$ and is of the form

$$\langle \Psi(\mathbf{X}) \rangle = \Psi(\mathbf{X_0}) + \sum_{i=1}^{m} \left\{ \langle (X_i - X_{0_i}) \rangle \frac{\partial \Psi}{\partial X_i}(\mathbf{X_0}) \right\} + \frac{1}{2!} \sum_{i=1}^{m} \sum_{j=1}^{m} \left\{ \langle (X_i - X_{0_i})(X_j - X_{0_j}) \rangle \frac{\partial^2 \Psi}{\partial X_i \partial X_j}(\mathbf{X_0}) \right\} + \cdots . \tag{9}$$

Here, $\mathbf{X_0} = \langle \mathbf{X} \rangle$, and consequently, the second term in the above equation is identically equal to zero. Further simplification in evaluation of $\langle \Psi(\mathbf{X}) \rangle$ is possible, if $\mathbf{X}$ is transformed into the standard normal space $\mathbf{U}$. If a complete knowledge of joint pdf of $\mathbf{X}$ is available, one can use the well-known Rosenblatt transformation to achieve this. On the other hand, when $\mathbf{X}$ is only partially specified, which is most often the case in practice, one can use the theory of Nataf's transformations [11,43] for this purpose. In the present study, we adopt the latter approach. We specifically assume that knowledge of $\mathbf{X}$ is restricted to its first-order marginal pdf and its covariance matrix. The transformation of $\mathbf{X}$, into the standard normal space $\mathbf{U}$, involves two steps. We first apply Nataf's memoryless transformation given by $X_i = \zeta_i^{-1}[\Phi_i(V_i)]$, where, $\zeta_i(\cdot)$ and $\Phi_i(\cdot)$ are, respectively, the marginal pdf of X_i and V_i, to transform the vector of correlated, non-Gaussian random variables $\mathbf{X}$ to a vector of correlated Gaussian random variables $\mathbf{V}$. The joint pdf of the normal variates, $p_{\mathbf{V}}(\cdot)$, is characterized by the unknown correlation coefficient matrix $\mathbf{C_V}$. The correlation coefficients $\mathbf{C}_{\mathbf{V}_{ij}}$ are expressed in terms of the known correlation coefficients $\mathbf{C}_{\mathbf{X}_{ij}}$ through an integral equation, which is solved by applying a search algorithm, to obtain $\mathbf{C_V}$ [40]. The vector of correlated Gaussian random variables $\mathbf{V}$ are related to the standard normal variates $\mathbf{U}$, through the expression $\mathbf{V} = \mathbf{L}\mathbf{U}$. Here, $\mathbf{L}$ is the lower triangular matrix, such that $\mathbf{C_V} = \mathbf{L}\mathbf{L}^t$. $\mathbf{L}$ is determined by Cholesky decomposition of $\mathbf{C_V}$. The m-dimensional extreme value distribution $\Psi(\mathbf{X})$, is now expressed as $\Theta(\mathbf{U})$, in the $\mathbf{U}$-space. Estimates of the unconditional extreme value distribution, is now expressed as

$$\langle \Theta(\mathbf{U}) \rangle = \Theta(\mathbf{U_0}) + \sum_{i=1}^{m} \left\{ \langle (U_i - U_{0_i}) \rangle \frac{\partial \Theta}{\partial U_i}(\mathbf{U_0}) \right\} + \frac{1}{2!} \sum_{i=1}^{m} \left\{ \langle (U_i - U_{0_i})^2 \rangle \frac{\partial^2 \Theta}{\partial U_i^2}(\mathbf{U_0}) \right\} + \cdots . \tag{10}$$

Here $U_{0_i} = \langle U_i \rangle = 0$, $(i = 1, \ldots, m)$. From Eqs. (9) and (10), it can be seen that transformation of the problem to the $\mathbf{U}$-space leads to the following advantages:

1. All moment terms $\langle U_i^p \rangle$, in Eq. (10), are identically equal to zero, when p is an odd integer.
2. Since $\langle U_i^p U_j^q \rangle = 0$ for $i \neq j$, where U_i and U_j are components of $\mathbf{U}$ and p, q are integers, one need not compute the cross-derivative terms such as $\partial^p \Theta(\mathbf{U}) / \Pi_{i=l}^{l+p} \partial U_i$ in Eq. (10).

3. If the gradients of $\Theta(\mathbf{U})$, with respect to U_i, are proposed to be evaluated numerically, Eq. (10) offers a few advantages; see Section 4.2.
4. Computation of higher-order expectations, $\langle U_i^{2p}\rangle$, $(p = 1, 2, \ldots)$, is easily achieved as U_i are standard normal random variables and it is well known that $\langle U_i^{2p}\rangle = (1)(3)\cdots(2p-1)\sigma^{2p}$, where $\sigma = 1$ is the standard deviation of U_i.
5. Also, since $\langle U_i^k\rangle/k! \to 0$ as $k \to \infty$, it ensures that the Taylors expansion is a convergent series if $\Theta(\mathbf{U})$ has continuous, finite derivatives up to the $(k+1)$th order in the interval under consideration.

In this context, it must be mentioned that the criterion for expanding $\Psi(\mathbf{X})$ as a Taylor series of k terms is that $\Psi(\mathbf{X})$ should have continuous finite derivatives up to the $(k+1)$th order in the interval under consideration [44].

4. Computing unconditional failure probability

In this section, we discuss techniques for computing P_f. Estimates of P_f, obtained from Eqs. (9) or (10), are subject to

(a) truncation errors, as finite number of terms are considered in the Taylor series expansion, and
(b) errors in computing the gradients appearing in Eqs. (9)–(10).

Thee accuracy of estimates of P_f can be improved by reducing these errors. With this in view, we discuss the following three methods for computing P_f.

4.1. Analytical approach

Errors in gradient calculations can be eliminated if closed-form expressions are obtained analytically for the gradients. For univariate/multivariate extreme value distributions, $\Psi(\mathbf{X})$ is a function of the PSD matrix of $\mathbf{Z}$. When $\mathbf{Z}$ is Gaussian, it can be shown that by applying the chain rule of differentiation, the computation of gradients of $\Psi(\mathbf{X})$, reduces to computing the gradients of the PSD matrix with respect to $\mathbf{X}$. Expressing in the frequency domain, the vector of response quantities of interest, we get from Eqs. (3)–(4),

$$\mathbf{D}(\omega)\mathbf{Z}(\omega) = \mathbf{F}(\omega). \tag{11}$$

Here, $\mathbf{D}(\omega) = \mathscr{D}(\omega)\mathscr{H}(\omega)$, $\mathscr{D}(\omega) = [-\omega^2\mathbf{M} + \mathrm{i}\omega\mathbf{C} + \mathbf{K}]$ and $\mathscr{H}(\omega) = [-\omega^2\mathbf{P} + \mathrm{i}\omega\mathbf{Q} + \mathbf{R}]^{-1}$ are functions of $\mathbf{X}$. $\mathbf{Z}(\omega)$ and $\mathbf{F}(\omega)$ are, respectively, the Fourier transforms of $\mathbf{Z}_0(t)$ and $\mathbf{F}_0(t)$, where $\mathbf{Z}_0(t) = \mathbf{Z}(t)$, $\mathbf{F}_0(t) = \mathbf{F}(t)$ for $0 < t < T_0$ and $\mathbf{Z}_0(t) = 0$, $\mathbf{F}_0(t) = 0$ for $t > T_0$; where $T_0 \to \infty$. Consequently, the PSDs of excitation and response are related through the equation

$$\mathbf{S_{FF}}(\omega) = \mathbf{D}(\omega)\mathbf{S_{ZZ}}(\omega)\mathbf{D}^*(\omega), \tag{12}$$

where the superscript, $*$, denotes complex conjugation. It must be noted that, for support motion problems, $\mathbf{S_{FF}}(\omega) = \mathbf{M}\boldsymbol{\Gamma}S_{gg}(\omega)\boldsymbol{\Gamma}^t\mathbf{M}$ and hence, is a function of $\mathbf{X}$. Here, $S_{gg}(\omega)$ denotes the PSD of the ground acceleration and $\boldsymbol{\Gamma}$ is the vector of influence factors. Differentiating both sides of Eq. (12) with respect to the components of $\mathbf{X}$, and taking $\partial\mathbf{S_{ZZ}}/\partial X_i$ on the left-hand side, it can be shown that

$$\mathbf{S}'_{\mathbf{ZZ}} = \mathbf{H}[\mathbf{M}'\boldsymbol{\Gamma}\mathbf{S_{gg}}\boldsymbol{\Gamma}^t\mathbf{M}^* + \mathbf{M}\boldsymbol{\Gamma}\mathbf{S_{gg}}\boldsymbol{\Gamma}^t\mathbf{M}^{*\prime} - \mathbf{D}'\mathbf{S_{ZZ}}\mathbf{D}^* - \mathbf{D}\mathbf{S_{ZZ}}\mathbf{D}'^*]\mathbf{H}^*. \tag{13}$$

Here $\mathbf{H} = \mathbf{D}(\omega;\mathbf{X})^{-1}$ and the operator $(')$ denotes partial derivative with respect to X_i. Assuming damping to be viscous and proportional, we express $\mathbf{C} = \alpha\mathbf{M} + \beta\mathbf{K}$, where α and β are, respectively, the mass and stiffness proportionality constants. Thus, from Eq. (13), it is observed that the first-order gradients of $\mathbf{S_{ZZ}}$, with respect to X_i, are expressible in terms of the first-order gradients of the mass and stiffness matrices, with respect to X_i. Similarly, by differentiating Eq. (12) with respect to X_i and X_j, analytical expressions for the second-order gradients of $\mathbf{S_{ZZ}}$ are obtained in terms of $\partial\mathbf{M}/\partial\mathbf{X}$, $\partial\mathbf{K}/\partial\mathbf{X}$, $\partial^2\mathbf{M}/\{\partial X_i\partial X_j\}$ and $\partial^2\mathbf{K}/\{\partial X_i\partial X_j\}$. Expressions for these quantities are obtained by analytical differentiation of the matrices $\mathbf{M}$ and $\mathbf{K}$, which are taken to be known explicitly. Following the chain rule of differentiation, expressions for higher-order gradients are

similarly determined. It must be noted that it is simpler to obtain analytical expressions for gradients of the conditional multivariate extreme value distributions, in the **X**-space than in **U**-space, and hence, Eq. (9) is used in computing estimates of the unconditional extreme value distribution. Analytical expressions for the gradients when structure nonlinear behavior is considered and/or when the transformation function $Q[\cdot]$ is nonlinear (in either case this implies that **Z** is non-Gaussian) are, ingeneral, difficult to determine.

4.2. Numerical approach

Deriving analytical expressions for gradients of conditional multivariate extreme value distributions, involve tedious algebra and can be a cumbersome process, especially for large structures and when the dimension of **X** is high. This difficulty can be circumvented, if numerical schemes are adopted for computing gradients. The problem of numerical evaluation of gradients have been widely studied, for example, in problems of computational fluid mechanics [45–47] and in problems of response surface-based structural reliability analyses [48–51]. We employ some of these techniques, in our studies, and explore their relative performance. In implementing these methods, it is found advantageous to work in the standard normal space and use the expression for P_f as given by Eq. (10), rather than Eq. (9). In the following sections, we discuss two techniques and these are applied later in the numerical examples, for computing gradients.

4.2.1. Central difference scheme

Most techniques, applied for gradient computations, are based on finite-difference approximations. Finite-difference equations for evaluating gradients of any order, up to a desired order of approximation, can be generated by evaluating the function to be differentiated, at sufficient number of points [46]. The order of approximation indicates how fast the error reduces as the grid is refined and does not indicate the absolute magnitude of error. Of the several finite-difference schemes available, the central difference scheme is preferred as, with a specified number of function evaluations, the order of approximation achieved is highest. Using the central difference scheme, the formulae for the first four derivatives of a function, $\zeta(U)$, with a fourth-order approximation, can be shown to be given by [46]

$$\zeta^{\mathrm{I}} = (\zeta_{i-2} - 8\zeta_{i-1} + 8\zeta_{i+1} - \zeta_{i-2})/12h + O(h^4),$$

$$\zeta^{\mathrm{II}} = (-\zeta_{i-2} + 16\zeta_{i-1} - 30\zeta_i + 16\zeta_{i+1} - \zeta_{i-2})/12h^2 + O(h^4),$$

$$\zeta^{\mathrm{III}} = (\zeta_{i-3} - 8\zeta_{i-2} + 13\zeta_{i-1} - 13\zeta_{i+1} + 8\zeta_{i-2} - \zeta_{i-3})/8h^3 + O(h^4),$$

$$\zeta^{\mathrm{IV}} = (\zeta_{i-3} + 12\zeta_{i-2} - 39\zeta_{i-1} + 56\zeta_i - 39\zeta_{i+1} + 12\zeta_{i+2} - \zeta_{i+3})/6h^4 + O(h^4). \tag{14}$$

Here the superscripts, in roman numerals, indicate the order of the gradient of ζ with respect to U, h represents the distance between successive grid points and ζ_{i+p}, $p = -3, \ldots, +3$, represents the numerical values of ζ, evaluated at $U + ph$. Thus, the use of Eqs. (14) for gradient computations, involves, the evaluation of $\zeta(U)$ at six other points, apart from the origin. In our studies, **U** is an m-dimensional vector and using Eq. (10) for estimating the unconditional failure probability requires that Taylor series expansion be carried out along each of the m-components of **U**. If terms only up to the fourth order are included in the Taylor series expansions, and, if Eqs. (14) are used to compute the gradients, $6m + 1$ evaluations of $\Theta(\mathbf{U})$ are required. It must be noted that in the limit $h \to 0$, Eqs. (14) lead to exact estimates for the gradients. However, in numerical calculations, too small values of h cause numerical instabilities, leading to erroneous estimates for the gradients. Thus, a judicious choice of h needs to be made for obtaining accurate estimates for the gradients. A procedure for choosing h has been discussed later in this paper.

4.2.2. Polynomial fitting

An alternative procedure of computing gradients, and which has been used in response surface-based reliability analyses [48–51], is to fit a polynomial for the function whose gradients we seek and subsequently, differentiate the polynomial at the desired location. It has been suggested [47] that the degree of the polynomial that is to be fitted, should be at least two orders more than the highest order derivative one wishes

to evaluate. In general, the order of truncation error of the approximation is the degree of the polynomial minus one, when the spacings of the grid are non-uniform and is equal to the degree of the polynomial, otherwise. A kth order polynomial can be fitted by evaluating the function at k locations, defined by the grid.

In our studies, we rewrite Eq. (10), as

$$\langle \Theta(\mathbf{U}) \rangle = \Theta(\mathbf{U_0}) + 1/2! \sum_{i=0}^{n} \sigma_{U_i}^2 \chi_i^{II} + 3/4! \sum_{i=0}^{n} \sigma_{U_i}^4 \chi_i^{IV} + \cdots + 2k + 1\text{th term}. \tag{15}$$

Here, $\chi_i = \sum_{j=0}^{2k} a_{ij} U_i^j$ is the projection of $\langle \Theta(\mathbf{U}) \rangle$ on the ith axis, and the superscripts denote the derivative of χ_i with respect to U_i. The unknown coefficients a_{ij}, $(i = 0, \ldots, n)$, $(j = 1, \ldots, 2k)$ are obtained from the relation

$$\begin{Bmatrix} a_{i_0} \\ a_{i_1} \\ .. \\ a_{i_{2k}} \end{Bmatrix} = \begin{bmatrix} 1 & U_{i_1} & U_{i_1}^2 & . & . & U_{i_1}^{2k} \\ 1 & U_{i_2} & U_{i_2}^2 & . & . & U_{i_2}^{2k} \\ . & . & . & . & . & . \\ 1 & U_{i_{2k}} & U_{i_{2k}}^2 & . & . & U_{i_{2k}}^{2k} \end{bmatrix}^{-1} \begin{Bmatrix} \Theta_{i_1} \\ \Theta_{i_2} \\ .. \\ \Theta_{i_{2k}} \end{Bmatrix}, \tag{16}$$

where, Θ_{i_j} are evaluated by running the structural analysis code when U_{i_j} is the jth grid point for the ith component of $\mathbf{U}$, with all other components being situated at the mean. In the standard normal space, the mean $\mathbf{U_0} = 0$, represents its origin. Once the coefficients are determined, the gradients of ξ_i at $\mathbf{U_0}$ are estimated by differentiating the polynomial $\sum_{j=0}^{2k} a_{ij} U_i^j$ appropriate number of times at $\mathbf{U_0}$. It must be noted that if the Taylor series expansions are truncated after the fourth-order terms, the degree of polynomial that needs to be fitted is at least 6. This would require a grid containing seven points along each of the independent axis U_i, $(i = 1, \ldots, m)$. Since the central point is the origin, the total number of function evaluations required, for a fourth-order accuracy, is $6m + 1$.

5. Numerical examples and discussions

The accuracy of the procedures described in the previous section are first examined through two numerical examples where the vector processes are Gaussian and one example where the response vector is non-Gaussian. In the first example, we consider a linear, randomly parametered, 11-storey building, under seismic excitations. The structure is assumed to fail if the top storey displacement exceeds a specified threshold, in a given interval of time. In the second example, we study a linear, randomly parametered, two-span bridge, subjected to differential seismic support motions. Here, the bridge is assumed to fail if the midpoint displacements, in either of the two spans, exceed specified threshold levels. Thus, this is a problem in series system reliability. In both these examples, function $Q[\cdot]$ (see Eq. (4)) relating the excitations and the response quantities of interest, $\mathbf{Z}$, is linear. The third example illustrates the applicability of the proposed framework when $Q[\cdot]$ is nonlinear. Here, we consider the stresses at a particular location in a linear structure under stationary, Gaussian excitations. Consequently, the stress components turn out to be stationary, Gaussian processes. The performance function is defined in terms of the Von Mises stress and the major principal stress, which are obtained as nonlinear functions of the stress components. A structural failure is defined to occur if the Von Mises stress or the major principal stress, exceeds specified threshold levels. Thus, this is a problem in series system reliability, where the response vector constitutes non-Gaussian random processes. In all these three examples, the failure probability estimates, obtained by the proposed method, are compared with those obtained from Monte Carlo simulations. In this study, we validate the applicability of the proposed method for estimating the unconditional failure probabilities and hence, Monte Carlo simulations are carried out on the conditional extreme value distributions. Only the random variables representing structure randomness, are digitally generated and conditional multivariate extreme value distributions are computed from extreme value theory. The ensemble mean is then determined to compute estimates for the unconditional failure probability. The approximations for the extreme value distributions have been examined earlier with respect to full-scale Monte Carlo simulations and have not been repeated here. Finally, we illustrate the applicability of the proposed method in estimating the seismic fragility of a piping network in a nuclear power plant.

5.1. Eleven-storey building under seismic excitation

In this example, we study the reliability of a 11-storey building under seismic excitations. Modelled as a shear building, the 11-storey building is assumed to have floor masses m_i and storey stiffnesses k_i, $(i = 1, \ldots, 11)$. It has been assumed that all the floors are identical with the mean values of m_i and k_i being respectively, 8.5790×10^4 kg and 2.1×10^8 N/m. A free vibration analysis of the 11-storey building, with the structure properties being assumed to be deterministic at their mean values, reveals that the first two natural frequencies of the structure are, respectively, 6.69 and 19.95 rad/s and the highest natural frequency is 97.12 rad/s. The structure damping is assumed to be viscous and proportional. The mass and stiffness proportionality constants, α and β, are assumed to have mean values $0.1428\,\mathrm{s}^{-1}$ and 0.0027 s, respectively. This corresponds to modal damping ratio of 1.97% in the first mode and 13.18% in the last mode, for the structure with mean properties. The structure parameters $m_1, \ldots, m_{11}, k_1, \ldots, k_{11}, \alpha$ and β are considered to be lognormally distributed random variables. For the sake of simplicity, it has been assumed that these random variables are mutually independent. Thus, $\mathbf{X}$ constitutes a vector of 24 random variables. The seismic acceleration is assumed to be a stationary, Gaussian random process, with a PSD function, defined as

$$S_{aa}(\omega) = S_0\omega_g^2(\omega_g^2 + 4\eta_g^2\omega^2)/\{(\omega_g^2 - \omega^2)^2 + (2\eta_g\omega\omega_g)^2\}. \tag{17}$$

Here, $\omega_g = 12.82$ rad/s, $\eta_g = 0.3$, ω is frequency and S_0 is a parameter that denotes the intensity of the excitations. The safety of the structure is defined in terms of the maximum displacement for the topmost storey, Δ_m, observed for a period of $T = 10$ s in the steady state. The structure is assumed to have failed if Δ_m exceeds the allowable top storey displacement, taken to be 0.125 m. Since linear structure behavior is assumed, the top storey displacement, conditioned on $\mathbf{X}$, in the steady state is a stationary, Gaussian random process. Estimates of the probability distribution of Δ_m, conditioned on $\mathbf{X}$, are obtained from extreme value theory of scalar Gaussian processes. Subsequently, the methods proposed in Section 4 are applied to obtain estimates for the unconditional failure probabilities.

As has been discussed earlier, estimates of P_f obtained by the proposed methods, are subject to errors due to series truncation and gradient computations. Guidelines to reduce these errors need to be evolved for accurate reliability estimates. With this in view, we first carry out a parametric study on the various computational aspects of the proposed method. For the sake of simplicity, we first assume that all 24 structure random variables exhibit identical coefficient of variation (cov). It is expected that if $\mathbf{X}$ exhibits large variations, we need to consider higher number of terms in the Taylor series expansions, in order to reduce errors due to truncation. This, in turn, would mean that higher-order gradients need to be computed. The numerical errors associated with computing gradients, however, are greater for higher-order gradients and can potentially, outweigh the advantage of including higher-order terms in the Taylor series. In order to study these aspects, we consider, three-, five- and seven-term Taylor series expansions. The gradients are computed by the three methods discussed earlier, namely, (a) analytically, (b) central difference scheme and (c) polynomial fitting approach. Estimates of P_f are obtained for various levels of coefficient of variation of $\mathbf{X}$. These predictions are compared with those obtained from limited Monte Carlo simulations carried out on 1000 samples and are illustrated in Fig. 1. Fig. 2 illustrates the absolute error of the estimates, expressed as a percentage of the Monte Carlo simulation predictions. It is seen from this figure, that the error in estimates of P_f, when the gradients are computed analytically, increases monotonically as coefficient of variation of $\mathbf{X}$ increase. This can be attributed to the fact that analytical computation of gradients are exact and the error has contributions only from truncation errors, which increases as coefficient of variation of $\mathbf{X}$ increases, when a fixed number of terms are considered in the Taylor series. On the other hand, when gradients are evaluated numerically, the error term has additional contributions from gradient computation errors, which, in turn, depend on the grid spacings. Too coarse or too fine grid spacings lead to unacceptable gradients. Table 1 illustrates how P_f estimates vary as the grid is made finer. It is obvious that a primary problem in the numerical approaches is to determine an acceptable grid. In this study, we adopt the following strategy to address

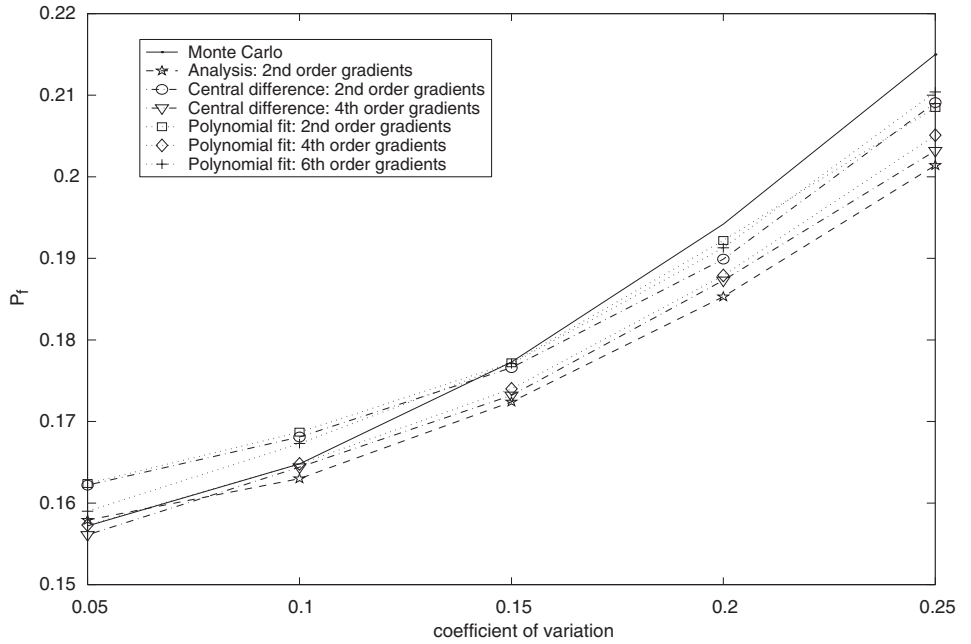

Fig. 1. Estimates of failure probability using proposed methods; example 1; note that, here, $P_{f|\mathbf{X}=\mathbf{x}_0} = 0.1544$.

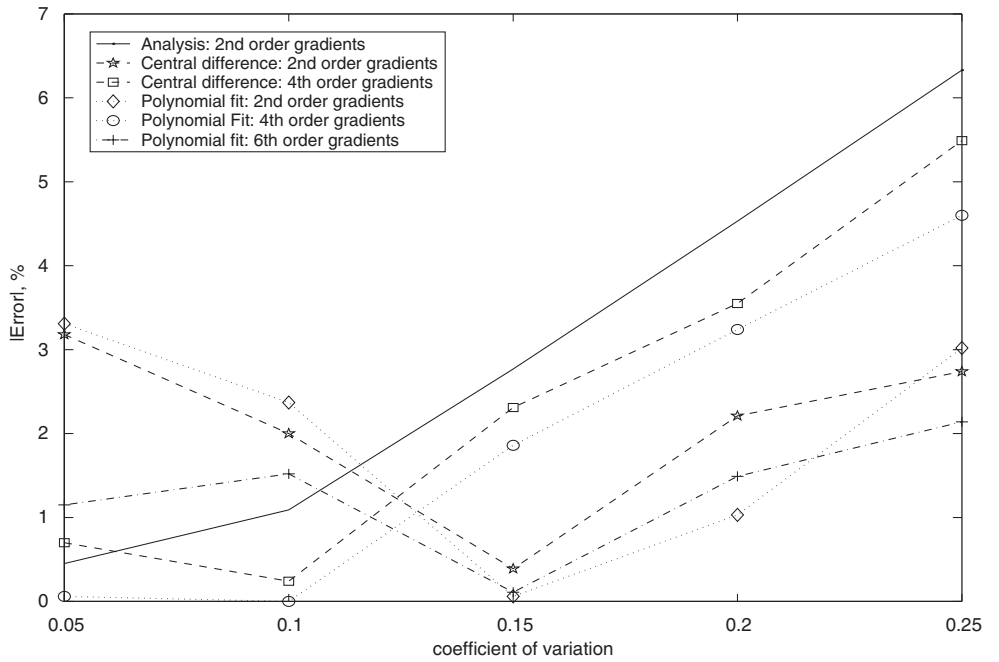

Fig. 2. Percentage error in prediction of P_f by the proposed methods, considering second-, fourth- and sixth-order gradients; example 1.

this problem:

(1) In the **X**-space, select the random variables which exhibit the highest coefficient of variation among the components of **X**. Transform only these random variables into the standard normal space. Assume the remaining structure properties to be deterministic at their mean levels.

Table 1
Variation of estimates of P_f with grid spacing

Grid spacing h	P_f				
	N_2	N_4	R_2	R_4	R_6
0.5	0.2285	0.0106	0.2337	0.0157	0.3257
0.6	0.2144	0.0919	0.2187	0.0962	0.2211
0.7	0.2038	0.1349	0.2071	0.1382	0.1897
0.8	0.1956	0.1570	0.1979	0.1594	0.1811
0.9	0.1893	0.1671	0.1910	0.1688	0.1785
1.0	0.1846	0.1711	0.1859	0.1724	0.1771
1.1	0.1813	0.1726	0.1823	0.1736	0.1761
1.2	0.1789	0.1732	0.1797	0.1740	0.1754
1.3	0.1774	0.1735	0.1781	0.1741	0.1749
1.4	0.1766	0.1735	0.1772	0.1741	0.1746
1.5	0.1761	0.1735	0.1767	0.1741	0.1745

N_2, second-order Taylor's expansion, gradients computed using central difference scheme; N_4, fourth-order Taylor's expansion, gradients computed using central difference scheme; R_2, second-order Taylor's expansion, gradients computed by fitting sixth-order polynomial; R_4, fourth-order Taylor's expansion, gradients computed by fitting sixth-order polynomial; R_6, sixth-order Taylor's expansion, gradients computed by fitting sixth-order polynomial; example 1; note that coefficient of variation of $\mathbf{X} = 0.15$, Monte Carlo simulations on 1000 samples yield $P_f = 0.1773$.

Table 2
Variation of converged grid spacing, for the proposed methods, with coefficient of variation of $\mathbf{X}$

Coefficient of variation	h				
	N_2	N_4	R_2	R_4	R_6
0.05	0.6	0.7	0.6	0.8	0.8
0.10	1.3	1.1	1.3	1.1	0.9
0.15	1.3	1.1	1.3	1.1	1.0
0.20	1.5	1.2	1.5	1.2	1.0
0.25	1.5	1.2	1.6	1.2	1.0

N_2, second-order Taylor's expansion, gradients computed using central difference scheme; N_4, fourth-order Taylor's expansion, gradients computed using central difference scheme; R_2, second-order Taylor's expansion, gradients computed by fitting sixth-order polynomial; R_4, fourth-order Taylor's expansion, gradients computed by fitting sixth-order polynomial; R_6, sixth-order Taylor's expansion, gradients computed by fitting sixth-order polynomial; example 1.

(2) Choose aninitial grid spacing h and compute P_{f_i}. The gradients may be computed using any of the numerical approaches discussed in this paper.
(3) Consider a new grid spacing $h + \delta$, where δ is a small number. Compute $P_{f_{i+1}}$ corresponding to the new grid.
(4) If the difference between P_{f_i} and $P_{f_{i+1}}$ exceed a prescribed tolerance ε, repeat steps (3–4) till convergence is achieved.
(5) For the converged grid, apply the proposed method by considering the effect of all the structure random variables, and estimate P_f.

It must be noted that estimates of P_f, listed in Table 1, have been computed when all 24 random variables exhibit identical coefficient of variation of 0.15 and hence, dimensional reduction was not possible in the pilot runs. In determining the grid size h, the tolerance ε, was taken to be $0.1P_{f_i}$. Table 2 lists the values of h when this criterion was satisfied, for various levels of coefficient of variation of $\mathbf{X}$ and when different methods were used in numerical computation of gradients. It is observed from this table, that the grid spacings depend as much on the

coefficient of variation of the random variables as on the method of computing the gradients. The criterion of choosing h does not take into account the rates of convergence and the direction of approach to the correct estimate and this accounts for the non-monotonous nature of the error plots, in Fig. 2, for the different numerical approaches. However, in general, it is observed that the accuracy of P_f estimates decrease as coefficient of variation increases. Based on the studies carried out, so far, the following remarks can be made:

(1) For higher coefficient of variation of $\mathbf{X}$, inclusion of higher-order terms in the Taylor series, so as to reduce truncation errors, do not necessarily lead to more accurate results. In most situations, reasonably accurate estimates are obtained when only second-order terms are considered in Taylor series expansions. This, however, implies that the coefficient of variation of $\mathbf{X}$ be within 25%.
(2) Though analytical computation of gradients are exact, in most applications, it is difficult to obtain analytical expressions for the gradients, thereby, limiting the scope of this approach.
(3) For grids involving the same number of points, estimates of P_f obtained when gradients are computed using the central difference scheme are of the same order of accuracy, as when polynomial fitting approach is used in computing derivatives.
(4) The coefficients for the polynomial to be fitted, are obtained by inverting a matrix in Eq. (16). The accuracy with which a matrix is inverted depends on its condition number. The inverse of the condition number has values ranging from 0.0 to 1.0, with a value closer to 1.0 representing a well-conditioned matrix, whose computed inverse can be assumed to have less numerical inaccuracies. Since the numerical differentiations are carried out in the $\mathbf{U}$-space, the mean vector $\mathbf{U_0}$ denotes the origin in the $\mathbf{U}$-space. This implies that the first row of the matrix in the right-hand side of Eq. (16) has zeros except for the first column. Moreover, due to the unique nature of the form of the matrix, and the location of the sampling points being defined symmetrically about the origin, the inverse of the condition number of the matrix, is maximum, when the grid spacing is equal to unity. From the pilot runs carried out in this study, to determine the grid spacings, we observe that indeed, the grid spacings are in the neighborhood of unity.

In this context, it is worth mentioning that in structural reliability based response surface literature, similar problems are faced in fitting polynomials around the design point. In most studies existing in the literature, the authors propose that considering the grid spacing to be between 1 and 3, lead to fairly accurate estimates [48–51].

5.2. Two span bridge under seismic excitations

In this example, we consider the reliability analysis of a randomly parametered two span bridge under seismic excitations. The two span bridge is idealized as a two span Euler–Bernoulli beam, with m being the mass per unit length and EI the flexural rigidity of the beam. The spans are assumed to be of length 55 and 45 m, respectively. Using the finite-element method, the structure is discretized into 40, 2-noded beam elements, with one translational and one rotational degrees of freedom per node. A free vibration analysis, when the structure properties are assumed to be deterministic at their mean values, revealed that the first five natural frequencies are 3.79, 6.70, 14.68, 22.37 and 32.49 Hz, respectively. The bridge, having three supports situated at large distances from each other, is assumed to be subjected to spatially varying earthquake accelerations with zero mean. Only the transverse components of the earthquake accelerations at the three supports are considered in the analysis and are specified through a 6×6 PSD matrix. The auto-PSD functions for the accelerations at the ith support, S_{ii}, is assumed to be of the form given in Eq. (17). Here, ω_g and η_g are assumed to be parameters that vary for each support depending on the local soil conditions. The seismic accelerations at the supports are assumed to have the same measure of intensity S_0. The information on the parameters ω_{g_i}, η_{g_i} and S_{0_i}, $(i = 1, 2, 3)$, are, however, assumed to be uncertain and are treated as random variables. The coherency function of the ground accelerations between any two supports $j, l, j \neq l$, $(j, l = 1, 2, 3)$ is of the form

$$\gamma_{jl}(\omega) = |\gamma_{jl}(\omega)| \exp[\mathrm{i}\Phi_{jl}(\omega)]. \tag{18}$$

Models for $|\gamma_{jl}(\omega)|$ and $\Phi_{jl}(\omega)$ are taken from the literature [52] and are given, respectively, by

$$|\gamma_{jl}(\omega)| = \tanh\{C(a_1 + a_2 D_{jl})[\exp\{C(b_1 + b_2 D_{jl})f\} + 1/3f^c] + 0.35\},$$

$$\Phi_{jl}(\omega) = -\mathrm{i}\,\log\{h_{jl}(\omega)\exp[\mathrm{i}\phi_{jl}(\omega)] + [1 - h_{jl}(\omega)]\exp[\mathrm{i}\theta(\omega)]\}, \tag{19}$$

where, $\phi_{jl}(\omega) = \omega D_{jl}/V, h_{jl}(\omega) = \{1 + (f/19)^4\}^{-1}$, $a_1 = 2.535$, $a_2 = -0.0118, b_1 = -0.115, b_2 = -8.37 \times 10^{-4}$, $c = -0.878$, $V = 500\,\mathrm{m/s}$, f is the frequency in Hz and D_{jl} is the distance between supports j and l.

The structure is analyzed separately for the dynamic and pseudo-static components of the midpoint displacements at the two spans. The safety of the bridge structure is assumed to be defined through the dynamic components of the midspan displacements $\Delta_1(t)$ and $\Delta_2(t)$, respectively. For the dynamic analysis, damping is assumed to be viscous and proportional. The mass and stiffness proportionality constants, α and β, are adjusted such that, for the structure with mean properties, the damping in the first two modes, η_1 and η_2, is 5% and are respectively taken to have values $0.4939S^{-1}$ and $2.9960 \times 10^{-5}\,\mathrm{s}$. Since the excitations at the supports are stationary, Gaussian random processes and linear behavior is assumed, $\Delta_1(t)$ and $\Delta_2(t)$, for large t, are also stationary, Gaussian random processes whose auto-PSD functions $[S_{\Delta_1\Delta_1}(\omega)$ and $S_{\Delta_2\Delta_2}(\omega)]$ and cross-PSD function $[S_{\Delta_1\Delta_2}(\omega)]$ are obtained as linear combinations of $S_{it}(\omega)$, $(i = 1, 2, 3)$. The coherence spectrum for Δ_1 and Δ_2 is expressed as $|\gamma(\omega)| = |S_{\Delta_1\Delta_2}(\omega)|/[S_{\Delta_1\Delta_1}(\omega)S_{\Delta_2\Delta_2}(\omega)]^{0.5}$.

The randomness in the system is expressed through a vector of 15 mutually uncorrelated lognormally distributed random variables, the details of which are listed in Table 3. The theory of multivariate extreme value distributions is used to obtain estimates of failure probability, conditioned on the system random variables, $\Psi(\mathbf{X})$, for a time period of observation $T = 15\,\mathrm{s}$. Estimates of unconditional failure probabilities are computed by considering three- and five-term Taylor series expansions for $\Theta(\mathbf{U})$. The derivatives of $\Theta(\mathbf{U})$, with respect to $\mathbf{U}$, are computed numerically, using the polynomial fit approach discussed earlier. These estimates are compared with those obtained from Monte Carlo simulations on the multivariate extreme value distributions, with an ensemble of 250 samples. As has been pointed out already, the Monte Carlo simulations are implemented on evaluation of $\langle\Psi(\mathbf{X})\rangle$, assuming the expression for $P_{f|\mathbf{X}}$ to be valid. The acceptability of models for $P_{f|\mathbf{X}}$, via Monte Carlo simulations, has been examined in another of our recent paper [28] and these details are not repeated here. In the earlier paper, the effect of structure randomness in reliability calculations had been ignored. In this example, we have considered the same parameters to facilitate a comparison on the reliability estimates due to the effect of considering uncertainties in the system parameters. A comparison of the failure probability estimates obtained as a function of the threshold displacements, have been tabulated in Table 4. It is observed that the estimates obtained by the proposed method are in good agreement with those obtained from Monte Carlo simulations. The estimates

Table 3
Distributional details of the system property random variables in example 2

Property	Probability distribution	Mean	Coefficient of variation
EI	Lognormal	$2.025 \times 10^9\,\mathrm{Nm}^2$	0.05
m	Lognormal	$50\,\mathrm{kg/m}$	0.03
η_1	Lognormal	0.05	0.10
η_2	Lognormal	0.05	0.10
ω_{g_1}	Lognormal	$10.81\,\mathrm{rad/s}$	0.05
ω_{g_2}	Lognormal	$9.99\,\mathrm{rad/s}$	0.05
ω_{g_3}	Lognormal	$9.55\,\mathrm{rad/s}$	0.05
η_{g_1}	Lognormal	0.60	0.10
η_{g_2}	Lognormal	0.55	0.10
η_{g_3}	Lognormal	0.50	0.10
S_{0_1}	Lognormal	$0.014\,\mathrm{m}^2/\mathrm{s}^2/\mathrm{rad}$	0.10
S_{0_2}	Lognormal	$0.014\,\mathrm{m}^2/\mathrm{s}^2/\mathrm{rad}$	0.10
S_{0_3}	Lognormal	$0.014\,\mathrm{m}^2/\mathrm{s}^2/\mathrm{rad}$	0.10

Table 4
Estimates of failure probability for various threshold levels α_1 and α_2 for example 2

Threshold (mm)	Method	$\alpha_1 = 8.4$	$\alpha_1 = 11.2$	$\alpha_1 = 14.0$	$\alpha_1 = 16.8$
$\alpha_2 = 4.8$	D	0.7566	0.4440	0.4318	0.4317
	N	0.7011	0.5004	0.4851	0.4848
	R	0.6953	0.4988	0.4844	0.4842
	M	0.6992	0.4938	0.4807	0.4845
$\alpha_2 = 6.4$	D	0.5074	0.0345	0.0164	0.0162
	N	0.5566	0.0962	0.0564	0.0557
	R	0.5540	0.0956	0.0559	0.0552
	M	0.5551	0.0979	0.0590	0.0561
$\alpha_2 = 8.0$	D	0.4974	0.0187	0.0004	0.0002
	N	0.5435	0.0504	0.0029	0.0018
	R	0.5418	0.0501	0.0030	0.0019
	M	0.5454	0.0510	0.0032	0.0025
$\alpha_2 = 9.6$	D	0.4973	0.0185	0.0002	1.2850×10^{-6}
	N	0.5433	0.0492	0.0012	1.8107×10^{-5}
	R	0.5416	0.0489	0.0012	2.6860×10^{-5}
	M	0.5445	0.0423	0.0015	1.8870×10^{-5}

D, deterministic system; N, fourth-order Taylor's expansion, derivatives computed using central difference scheme; R, fourth-order Taylor's expansion, derivatives computed by fitting a sixth-order polynomial; M, Monte Carlo simulations.

corresponding to the five-term expansion are observed to be in better agreement, though marginally, with those obtained from Monte Carlo simulations.

5.3. Non-Gaussian response quantities in a linear structure under Gaussian excitations

In this example, we examine the applicability of the proposed method when $Q[\cdot]$ in Eq. (4) is nonlinear. We consider a linear structure under zero-mean, stationary, Gaussian excitations. The structure is modelled as a plane-stress problem. Consequently, at a particular location of the structure, the stress components, $\{Y_j(t)\}_{j=1}^3$, which when conditioned on system randomness, constitute a vector of mutually correlated, stationary Gaussian processes. Here, $Y_1(t)$ and $Y_2(t)$ denote the normal stress components and $Y_3(t)$ is the shear stress component. The auto- and cross-PSD of $\{Y_j(t)\}_{j=1}^3$ can be determined from a random vibration analysis of the linear structure. However, for the sake of illustration of the proposed method, in this example we omit details regarding the random vibration analysis of the structure. Instead, we assume that the auto- and cross-PSDs of $\{Y_j(t)\}_{j=1}^3$ are respectively, of the form

$$S_{jj}(\omega) = \frac{s_j^2}{\sqrt{\pi\alpha_j}} \exp\left[-\frac{\omega^2}{4\alpha_j}\right], \quad j = 1, 2, 3, \tag{20}$$

and

$$S_{jk}(\omega) = c_{jk}(\omega)\sqrt{S_{jj}(\omega)S_{kk}(\omega)}\exp[-\mathrm{i}\gamma_{jk}(\omega)], \quad j \neq k. \tag{21}$$

Here, s_j, $(j = 1, 2, 3)$ denote the measure of the intensity of the random processes $Y_j(t)$, $(j = 1, 2, 3)$, $\gamma_{jk}(\omega) = \omega/\psi_{jk}$ are the phase spectra with ψ_{jk} being constants and c_{jk} are the coherence spectra between processes $Y_j(t)$ and $Y_k(t)$. $c_{jk}(\omega)$ is assumed to be constant for all ω. A failure is defined to occur if the square of the Von Mises stress $\mathscr{V}(t)$ or the major principal stress $\mathscr{U}(t)$ exceeds their respective threshold levels, α_1 and α_2, in a specified time duration T. Here,

$$\mathscr{V}(t) = Y_1^2(t) + Y_2^2(t) + 3Y_3^2(t) - Y_1(t)Y_2(t), \tag{22}$$

Table 5
Distributional details of the system property random variables in example 3

Property	Probability distribution	Mean	Coefficient of variation
s_1	Lognormal	$3\sqrt{2}$	0.10
s_2	Lognormal	$6\sqrt{2}$	0.10
s_3	Lognormal	$3\sqrt{2}$	0.10
c_{12}	Lognormal	0.50	0.05
c_{13}	Lognormal	0.15	0.05
c_{23}	Lognormal	0.30	0.05
ψ_{12}	Lognormal	4	0.10
ψ_{13}	Lognormal	8	0.10
ψ_{23}	Lognormal	6	0.10

$$\mathscr{U}(t) = \frac{1}{2}\left[Y_1(t) + Y_2(t) + \sqrt{Y_1^2(t) + Y_2^2(t) - 2Y_1(t)Y_2(t) + 4Y_3^2(t)}\right]. \tag{23}$$

$\mathscr{V}(t)$ and $\mathscr{U}(t)$ are obtained as nonlinear transformations of $\{Y_j(t)\}_{j=1}^3$ and are, thus, non-Gaussian processes. The failure probability is given by

$$P_f = 1 - P[\{\mathscr{V}_m\langle\alpha_1\} \cap \{\mathscr{U}_m\langle\alpha_2\}], \tag{24}$$

where $\mathscr{V}_m = \max_{0\leqslant t\leqslant T}\mathscr{V}(t)$, $\mathscr{U}_m = \max_{0\leqslant t\leqslant T}\mathscr{U}(t)$ and $T = 10\,\text{s}$. The system randomness is assumed to be reflected through the parameters in Eqs. (20), (21). We consider $\mathbf{X}$ to constitute a nine-dimensional vector of mutually uncorrelated, lognormal distributed random variables, the details of which are illustrated in Table 5.

In evaluating P_f from Eq. (24), we first approximate the joint extreme value distribution for $\mathscr{V}(t)$ and $\mathscr{U}(t)$, conditioned on $\mathbf{X}$, using the recently developed theory of multivariate extreme value distributions for nonlinear transformations of vector Gaussian processes [30]. Briefly stated, this theory is built on the assumption that for high thresholds, the level crossings of non-Gaussian processes can be modelled as Poisson point processes. The expressions relating the extreme value distributions for vector processes to their joint mean out-crossing rate have been discussed earlier [28]. This implies that one needs to develop approximations for $\langle N_1\rangle$, $\langle N_2\rangle$ and $\langle N_1N_2\rangle$, where N_1 and N_2 are the number of level crossings by $\mathscr{U}$ and $\mathscr{V}$, across their respective threshold levels, α_1 and α_2, in time $[0, T]$. It is well known from Rice's formula [4] that the mean rate of level crossings are related to the joint pdf of the process and their instantaneous time derivative, which for scalar and vector processes, are given respectively by,

$$\langle N_i\rangle = \int_0^T \int_0^\infty \dot{u}p_{Z_i\dot{Z}_i}(\alpha_i, \dot{u}; t)\,\mathrm{d}\dot{u}\,\mathrm{d}t, \quad i = 1, 2, \tag{25}$$

and

$$\langle N_1N_2\rangle = \int_0^T \int_0^T \left\{\int_0^\infty \int_0^\infty \dot{u}\dot{v}p_{Z_1\dot{Z}_1Z_2\dot{Z}_2}(\alpha_1, \alpha_2, \dot{u}, \dot{v}; t_1, t_2)\,\mathrm{d}\dot{u}\,\mathrm{d}\dot{v}\right\}\mathrm{d}t_1\,\mathrm{d}t_2. \tag{26}$$

In this example, Z_1 and Z_2 respectively represent $\mathscr{U}$ and $\mathscr{V}$, at time t. The crux of the problem lies in developing approximations for $p_{Z_i\dot{Z}_i}(\cdot)$ and $p_{Z_1Z_2\dot{Z}_1\dot{Z}_2}(\cdot)$, which are in general, not known when $Q[\cdot]$ (see Eq. (4)) is nonlinear. With reference to this example, it can be shown that

$$\begin{aligned} p_{Z_i\dot{Z}_i}(\alpha_i, \dot{z}) &= \int_{-\infty}^\infty \int_{-\infty}^\infty p_{Y_2Y_3Z_i\dot{Z}_i}(y_2, y_3, \alpha_i, \dot{z})\,\mathrm{d}y_2\,\mathrm{d}y_3 \\ &= \sum_{j=1}^k \left\{\int_{\Omega_j} \cdots \int J_j^{-1} p_{\dot{Z}_i|Y_1Y_2Y_3}(\dot{z}|y_1, y_2, y_3) p_{Y_1Y_2Y_3}(y_1^{(j)}, y_2, y_3)\,\mathrm{d}y_2\,\mathrm{d}y_3\right\}, \end{aligned} \tag{27}$$

where, $J_j = |\partial Q/\partial Y_1|_j$, $p_{Y_2Y_3Z_i\dot{Z}_i}(y_2, y_3, \alpha_i, \dot{z}) = \sum_{j=1}^k |\partial Q/\partial Y_1|_j^{-1} p_{Y_1Y_2Y_3\dot{Z}_i}(y_1^{(j)}, y_2, y_3, \dot{z}_i)$ and Ω_j denotes the domain of integration determined by the permissible set of values y_2, y_3, for each solution of $y_1^{(j)}$ corresponding

to the nonlinear equation $Z_i = Q[Y_1, Y_2, Y_3]$, for $Z_i = \alpha_i$. Since $\mathbf{Y}(t)$ is Gaussian, $p_{Y_1Y_2Y_3}(\cdot)$ is a Gaussian density function. It can be shown that $\dot{Z}|_{\mathbf{Y}}(t)$ is expressible as a linear sum of $\dot{\mathbf{Y}}(t)$. This implies that, for a given t, $p_{\dot{Z}_i|Y_1Y_2Y_3}(\cdot)$ is Gaussian whose parameters can be easily determined. Numerical techniques for approximating $p_{Z_i\dot{Z}_i}(\cdot)$ from Eq. (27) have been discussed in Ref. [30]. Following similar principles of transformation for the vector case, it can be shown that for a bivariate vector $\mathbf{Z} = [Z_1, Z_2]$, we get

$$p_{Z_1Z_2\dot{Z}_1\dot{Z}_2}(\alpha_1, \alpha_2, \dot{z}_1, \dot{z}_2) = \int_{-\infty}^{\infty} p_{Y_3Z_1Z_2\dot{Z}_1\dot{Z}_2}(y_3, \alpha_1, \alpha_2, \dot{z}_1, \dot{z}_2)\,\mathrm{d}y_3 = \sum_{j=1}^{k}\left\{\int_{\Omega_j} \mathbf{J}_j^{-1} p_{\dot{Z}_1\dot{Z}_2|Y_1Y_2Y_3}(\dot{z}_1, \dot{z}_2|y_1, y_2, y_3) p_{Y_1Y_2Y_3}(y_1^{(j)}, y_2^{(j)}, y_3)\,\mathrm{d}y_3\right\}. \quad (28)$$

It is to be noted that $\mathbf{J}$ in Eq. (28) is a Jacobian matrix. Implicit in these transformations is the assumption that $p_{Z_1Z_2|Y_3}(\cdot) \perp p_{\dot{Z}_1\dot{Z}_2|Y_3}(\cdot)$. The accuracy of the approximations for the extreme value distributions determined from Eqs. (27)–(28), when system randomness is ignored, have been examined in Ref. [30] and is not repeated here.

Estimates of the unconditional failure probabilities are computed by considering three-term Taylor series expansions for $\Theta(\mathbf{U})$. As in the previous example, the derivatives of $\Theta(\mathbf{U})$, with respect to $\mathbf{U}$, are computed numerically, using the central difference scheme. These estimates are compared with those obtained from Monte Carlo simulations, with an ensemble of 500 samples. A comparison of the failure probability estimates have been tabulated in Table 6 and a fairly good agreement is observed with those from Monte Carlo simulations.

It is to be noted that in this example, the stress components are Gaussian and the nonlinear transformation $Q[\cdot]$, relating $\mathscr{V}(t)$ and $\mathscr{U}(t)$ with these components, is available explicitly. This has been possible since structure is assumed to be linear. On the other hand, if structure nonlinear behavior is considered, $Q[\cdot]$, in general, is not available in explicit form. In such situations, a response surface-based strategy may be used to develop approximations for the nonlinear transformation $Q[\cdot]$ relating the response quantities of interest with the Gaussian excitation components. This strategy, however, has not been explored in the present study.

5.4. Seismic fragility analysis of a pipeline in a nuclear power plant

The proposed method is now implemented to construct the fragility curves for a piping structure, in a seismically loaded nuclear plant. The earthquake ground accelerations, specified at the reactor base level, are

Table 6
Estimates of failure probability for various threshold levels α_1 and α_2, for example 3

Threshold (N/mm^2)	Method	$\alpha_1 = 755$	$\alpha_1 = 1289$	$\alpha_1 = 1644$	$\alpha_1 = 2000$
$\alpha_2 = 20.56$	D	0.9997	0.8757	0.8330	0.8285
	N	0.9332	0.6878	0.6779	0.6716
	M	0.9304	0.6844	0.6822	0.6812
$\alpha_2 = 28.89$	D	0.9052	0.1394	0.0393	0.0297
	N	0.8960	0.1703	0.0528	0.0481
	M	0.8922	0.1776	0.0592	0.0532
$\alpha_2 = 34.44$	D	0.8963	0.1127	0.0125	0.0028
	N	0.8916	0.1681	0.0240	0.0066
	M	0.8911	0.1602	0.0244	0.0076
$\alpha_2 = 40$	D	0.8956	0.1106	0.0103	6.9230×10^{-4}
	N	0.8894	0.1548	0.0223	0.0026
	M	0.8903	0.1586	0.0218	0.0030

D, deterministic system; N, second-order Taylor's expansion, derivatives computed using central difference scheme; M, Monte Carlo simulations.

modelled as a vector of stationary, Gaussian random processes and are characterized through the PSD matrix, defined along the principal components of the seismic excitations. The principal axes system is taken to be inclined at an angle of 21° on the horizontal plane to the coordinate system in which the reactor structure is modelled.

In the analysis procedure adopted, the reactor building and the piping structure are, respectively, assumed to be the primary and secondary systems. Finite element (FE) method is used to model these structures. The reactor building of the nuclear power plant is represented as a stick model; see Fig. 3. The FE stick model consists of 705 degrees of freedom (dof). An eigenvalue analysis on the stick model reveals that the first 65 modes lie within the spectrum range of the excitations, which, in turn, is taken to be in the range $[0, 36]$ Hz. A random vibration analysis of the stick model leads to the PSD matrix for the absolute accelerations along the six components, at the node where the piping structure is connected. To compute the absolute acceleration response, the dof corresponding to the reactor base along which the ground accelerations act, are released and large masses are added along these dofs. The large mass is taken to be 1×10^6 times the total mass of the reactor. This mass, in turn, is subjected to an equivalent force equal to the large mass multiplied by the applied seismic ground accelerations. A response analysis that includes the effect of rigid body modes leads to the determination of the absolute acceleration response. The FE model of the piping structure, shown in Fig. 4, consists of 2958 degrees of freedom. An eigenvalue analysis of the piping structure reveals that the first 74 natural frequencies lie in the frequency range of [0–36] Hz. The components of the PSD matrix of the seismic ground accelerations, aligned along the structure axes system, have been computed from on field data analysis. Here, the vertical component (along Y-axis) turns out to be independent of the other two components. A random vibration analysis is carried out to determine the auto- and cross-PSD functions for the absolute ground accelerations at the piping floor level. It must be noted that at the piping floor level, all the three displacement components are mutually correlated.

The failure modes for the piping structure have been defined with respect to the failure of its supporting structures. These supports are assumed to fail on initiation of yielding due to the bending stresses at the root of the supports exceeding permissible limits. The piping system under study has 21 such supports. In the FE model used for response analysis, these supports are represented as a set of discrete linear springs. The PSD of the transverse forces imparted on the supports by the pipes due to earthquake loading are computed using random vibration analysis on the piping structure FE model. These PSDs are used as inputs in the random vibration analysis on the supports. The supports have been modelled as cantilever beams. Since the pipes are

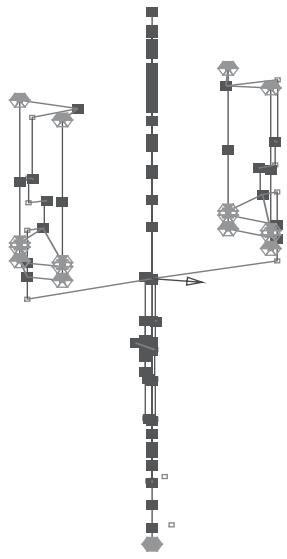

Fig. 3. FE stick model for the reactor building of the nuclear plant; the arrow indicated in the figure represents the location of the piping structure and the node for which the PSD matrix of absolute accelerations for the floor response are calculated.

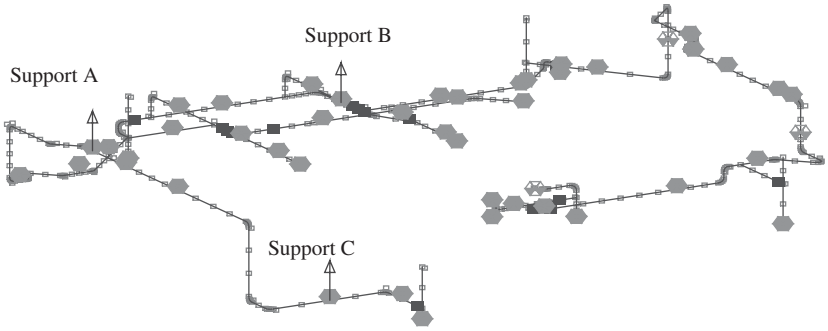

Fig. 4. FE model for the piping structure of the nuclear plant; the arrows indicated in the figure represent the location of the supports A, B and C.

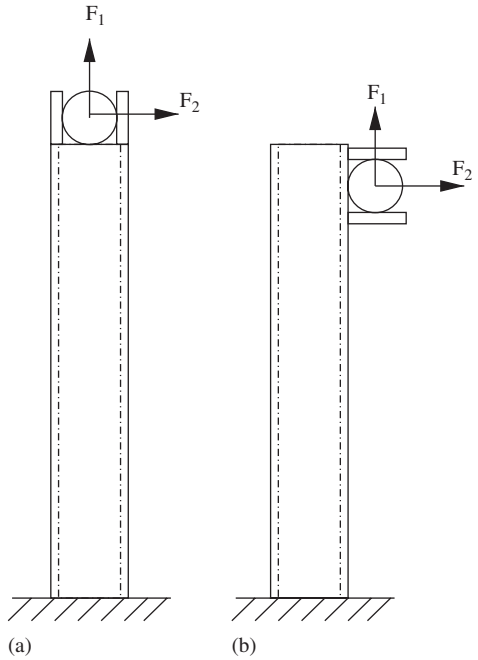

Fig. 5. Typical supports for the fire water pipeline: (a) Type 1, pure axial stress due to F_1 and bending stress due to F_2 and (b) Type 2, axial stress due to F_1, bending stresses due to F_1 and F_2.

not restrained axially, no forces acting along the axis of the pipe are imparted on the supports. Thus, the supports are subjected to two in-plane forces, F_1 and F_2 at their free ends. Depending on the configuration of the supports, they can be classified, primarily, under two types, see Fig. 5. In type 1 supports, the stress developed at the root of the supports have contributions from the axial stress due to F_1 and bending stress due to F_2. In supports of type 2, owing to the eccentricity of F_1, there is an additional bending stress due to F_1. Here, $F_1(t)$ and $F_2(t)$ are correlated, stationary, random processes. Since linear structure behavior is assumed, the excitations turn out to be stationary, Gaussian random processes and the stress developed at the root of the ith support ($i = 1, \ldots, 21$), $\sigma_i(t)$, is also a stationary, Gaussian random process, when conditioned on $\mathbf{X}$ and $\mathbf{\Theta}$. Here, $\mathbf{\Theta}$ is the vector of random variables representing the epistemic uncertainties. For the sake of illustration, it is assumed that the influence of uncertainties in loads and structural properties, on structural reliability, is much stronger than $\mathbf{\Theta}$. Denoting by $V_{M_i} = \max_{0 \leqslant t \leqslant T} \sigma_i(t)$, the performance function is written as $g_i[\{\ddot{\mathbf{U}}_g, \mathbf{X}, \mathbf{\Theta}\}] = C_i - V_{m_i}$ and $P_{f_i|\mathbf{X},\mathbf{\Theta}} = 1 - P[g_i[\{\ddot{\mathbf{U}}_g, \mathbf{X}, \mathbf{\Theta}\} \leqslant 0 \ \forall t \in (0, T)]$. Here, T is taken to be 20 s. The available limit stress $C_i = \sigma_{Y_i} - \sigma_{D_i} - \sigma_{T_i}$, where, σ_{Y_i}, σ_{D_i} and σ_{T_i} are, respectively, the permissible yield

stress, stress due to dead loads and stress due to thermal loads. Estimates of $P_{f_i|\mathbf{X},\mathbf{\Theta}}$ can be obtained from the well-known relation

$$P_{f_i|\mathbf{X},\mathbf{\Theta}} = 1 - \exp\left[\frac{T}{2\pi}\frac{\sigma_{\dot{V}}}{\sigma_V}\exp\left\{-0.5\left(\frac{C_i}{2\sigma_v}\right)^2\right\}\right]. \tag{29}$$

The structure uncertainties in the reactor building and the piping structure are modelled through a vector of mutually independent, lognormally distributed random variables $\mathbf{X}$. The guidelines provided in the JCSS document [1] are used, to the extent possible, to quantify the parameters of these random variables. It has been assumed that the dynamic characteristics of the reactor building and the supporting soil are prone to random fluctuations, which, in turn, affect the definition of the response of floors on which the secondary systems are connected. The damping model used for the reactor structure is as per the provisions stated in Ref. [53]. The stick model for the reactor is made up of six materials as listed in Table 7. The material damping constants associated with the materials are treated as a set of random variables with properties as given in Table 7. The properties considered random in the piping structure and their probabilistic properties are listed in Table 8. The coefficient of variation of the capacity of each structure is assumed to be 0.05. The mean capacity for each support varies and is taken to be the available limit stress, C_i, $(i = 1, \ldots, 21)$. Thus, in this study, the structure uncertainties is represented through a 10-dimensional vector $\mathbf{X}$. For the purpose of illustration, $\mathbf{\Theta}$ is assumed to constitute a 11-dimensional vector of mutually independent, lognormal random variables with unit mean. The corresponding coefficient of variations for Θ_i is listed in Table 9. Due to the multiplicative regeneracy property of lognormal random variables, these epistemic uncertainties lead to a lognormal model for Θ_0, given by $\Theta_0 = \{\Pi_{s=n_s+1}^{n_q}\Theta_s\}/\{\Pi_{s=1}^{n_s}\Theta_s\}$, where $\{\Theta_s\}$, $s = 1, \ldots, n_s$ are the randomvariables that represent the epistemic uncertainties in specifying the load effects and $\{\Theta_s\}$, $s = n_s + 1, \ldots, n_q$ are the random variables that represent the uncertainties in specifying structural capacities. In this example, Θ_0 is found to have mean 1.0 and coefficient of variation (cov) equal to 0.15. Some of the data on the cov of the epistemic uncertainty variables, listed in Table 9, have been taken from the literature [1]. Due to the lack of available data, the cov of the remaining random variables, listed in Table 9, have been assigned suitably.

As a first step, the values of $P_{f|\mathbf{X},\mathbf{\Theta}}$, have been computed for all 21 supports when the peak ground acceleration (pga) level corresponds to the maximum pga level which enables shutting down of a nuclear plant safely. This is characterised by ζ_g which is the measure of severity of ground excitations. For the safe

Table 7
Probabilistic properties of the damping ratios for the various materials in the reactor building model

Damping ratio of	Probability distribution	Mean	Coefficient of variation
Concrete Type 1	Lognormal	0.07	0.25
Concrete Type 2	Lognormal	0.05	0.25
Steel	Lognormal	0.03	0.25
Soil (translation in X direction)	Lognormal	0.30	0.25
Soil (translation in Y direction)	Lognormal	0.29	0.25
Soil (rotation)	Lognormal	0.44	0.25

Table 8
Details of properties considered random in the piping structure

Property	Probability distribution	Mean	Coefficient of variation
Young's modulus, E	Lognormal	2.018×10^5 N/m^3	0.03
Material density, ρ	Lognormal	7.883×10^3 kg/m^3	0.07
Damping ratio	Lognormal	0.02	0.30

Table 9
Details of modelling uncertainties

Source of modelling uncertainty	Coefficient of variation
Sampling fluctuations	0.05
Noise in measurements	0.05
Scaling effects from laboratory to field	0.05
Assumption on model for damping	0.10
Poisson approximation for determining extremes	0.05
Assumption on structure linear behavior	0.10
Assumptions on the orientation of the principal seismic excitations	0.05
Effects of primary–secondary structure interactions	0.05
Characterization of PSD matrix for principal seismic components	0.05
FE discretization	0.05
Modal truncation errors	0.02

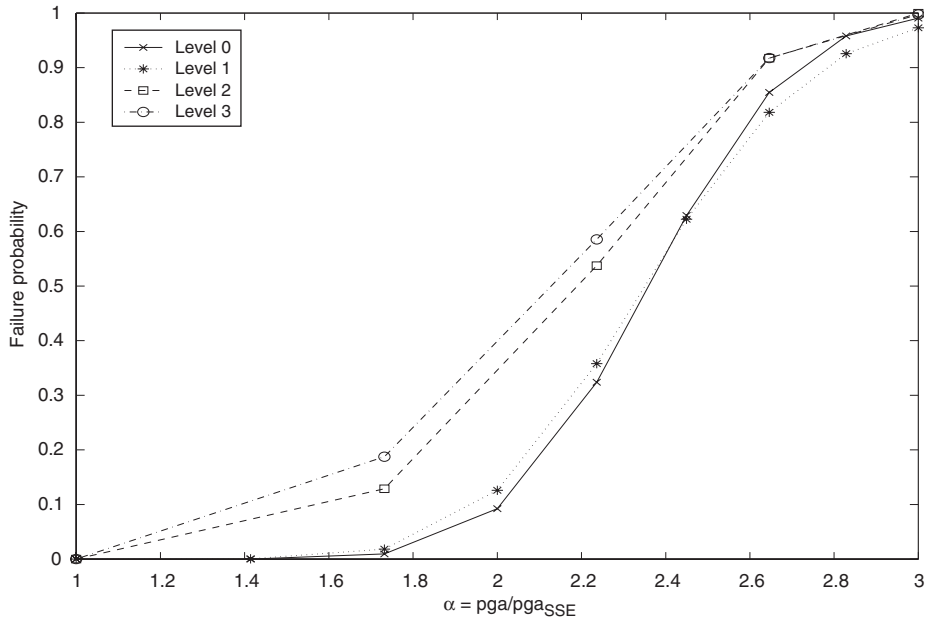

Fig. 6. Fragility curves for support A.

shut down earthquake (SSE), $\zeta_g = 0.2g$. It is observed that the estimated $P_{f|\mathbf{X},\boldsymbol{\Theta}}$ for three supports, A, B and C (see Fig. 4), are significantly higher than the rest at ζ_g. We retain only these three failure modes in further analysis. The mean values of the capacity for supports A, B and C are, respectively, 231.8, 210.0 and 235.1 $\mathrm{N/m^2}$.

For the sake of clarity, we introduce a nomenclature for the fragility curves. We term Level 0 fragility curves to be those conditioned on $\mathbf{X}$, $\boldsymbol{\Theta}$ and capacity. Level 1 and Level 2 fragility curves refer to the failure probability curves $P_{f|\mathbf{X},\boldsymbol{\Theta}}$ and $P_{f|\boldsymbol{\Theta}}$ respectively, while the unconditional failure probability curves versus ζ_g are termed as the Level 3 fragility curves. The Level 0 and Level 1 fragility curves for supports A, B and C are illustrated in Figs. 6–8. The excitation levels are represented in terms of pga, normalized with respect to the pga at SSE and is designated as $\alpha = \mathrm{pga}/\mathrm{pga}_{\mathrm{SSE}}$. It must be noted that the failure modes for supports A, B and C are mutually correlated. We assume that the failure of the pipeline occurs if any of these three supports fail. This implies a series system configuration for the failure modes. We employ the theory of multivariate extreme value distribution [28] to estimate the joint failure probability. The Level 1 fragility curve for the piping

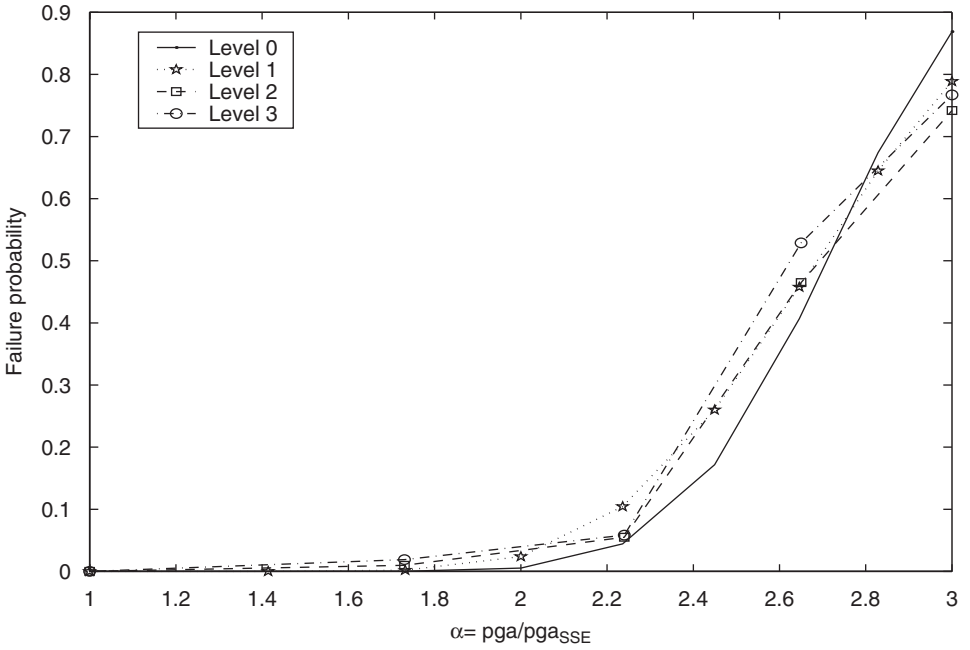

Fig. 7. Fragility curves for support B.

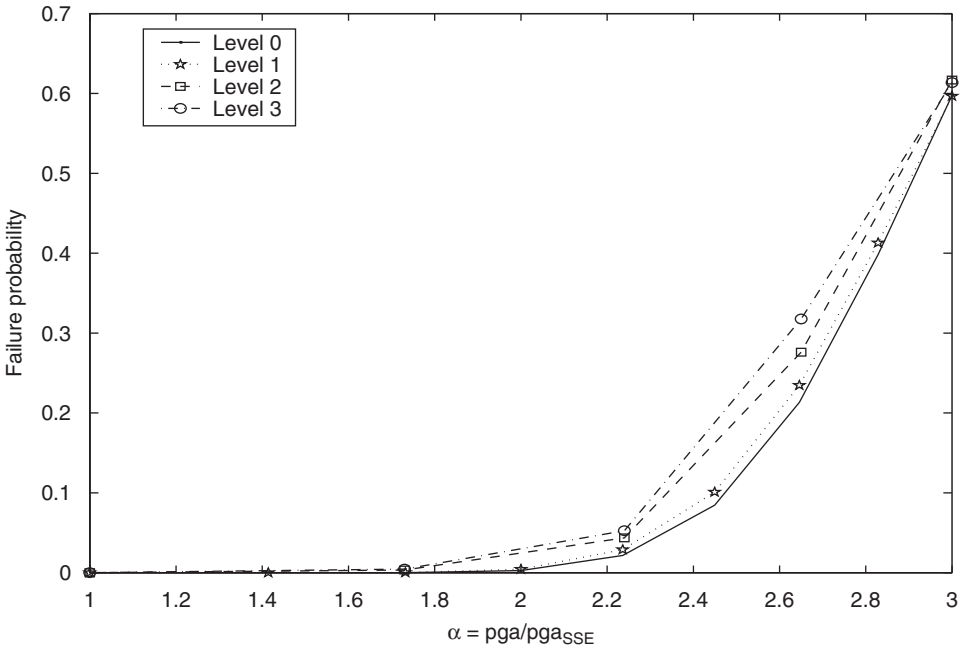

Fig. 8. Fragility curves for support C.

structure, obtained using the theory of multivariate extremes, is illustrated in Fig. 9. These are compared with the lower bound and upper bound level 1 fragility curves, given by [54]

$$\max_{1\leqslant i\leqslant n_k}[P_{f_i|\mathbf{X},\boldsymbol{\Theta}}]\leqslant P_{f|\mathbf{X},\boldsymbol{\Theta}}\leqslant 1-\Pi_{i=1}^{n_k}[1-P_{f_i|\mathbf{X},\boldsymbol{\Theta}}], \tag{30}$$

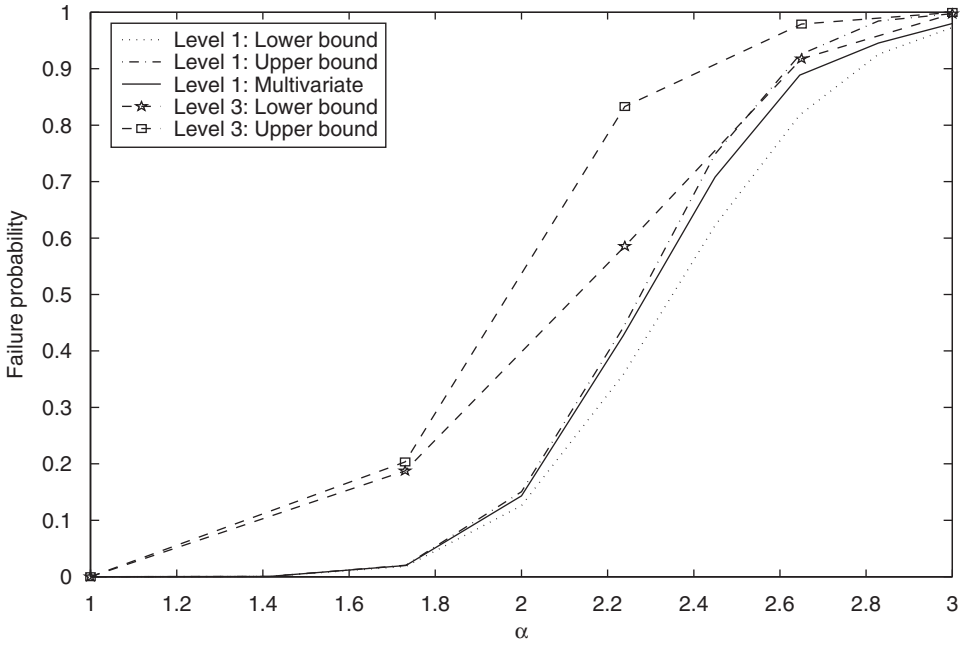

Fig. 9. Fragility curves for the piping structure.

where, $n_k = 3$ for this example. It is observed that at higher levels of excitations, the difference in the bounds for the failure probability estimates of the structure, is about 10%. In estimating both the system and component fragility curves, we make the assumption that the threshold crossings of the relevant random processes can be modelled as Poisson point processes. It is well known that the accuracy of the Poisson's approximation depends on the spectral bandwidth of the random processes. Since the system fragility curve obtained from the theory of multivariate extremes, lie within the bounds (see Fig. 9), it can be argued that errors associated in modelling the multivariate extreme value distribution, are, at worst, commensurate with those obtained from existing methods.

The Level 2 and Level 3 fragility curves are computed for the three supports and are illustrated in Figs. 6–8. It is observed that the difference in Level 1 and Level 2 fragilities is significant for low intensities of excitation. This seems to imply that structure randomness shows a stronger effect on the reliability of structures, especially for lower intensity excitations. This stands to reason since for a structure to fail under low-intensity excitations, the variability in the structural parameters becomes more important. On the other hand, the difference between Level 2 and Level 3 fragilities are almost of the same order at all excitation levels. This suggests that epistemic uncertainties induce a systematic error, which remains largely unaffected by the excitation intensities and depends only on the nature of these uncertainties. The bounds for the Level 3 fragility curves for the piping structure are also shown in Fig. 9. Here too, we observe that the difference in Level 3 and Level 1 fragilities to be large, in lower intensity excitations.

6. Conclusions

A framework for reliability analysis of randomly parametered vibrating structures, under random excitations, has been developed. The uncertainties associated with the problem are classified into three categories—those associated with the loadings, capacities and in structure properties, respectively. The proposed method is built on the assumption that the uncertainties in the loadings and the capacities have a predominant effect on the reliability of the structure. The loads are modelled as vectors of mutually correlated, Gaussian random processes. The structure properties and the capacities are modelled as a vector of mutually correlated, non-Gaussian random variables. The structural reliability, conditioned on the structure property

randomness, is estimated first, using theories of random processes and recently developed approximations for multivariate extreme value distributions. These approximations have been derived for vector Gaussian processes and for vector non-Gaussian processes, which can be expressed as nonlinear functions of vector Gaussian processes. Subsequently, the effect of structure randomness is incorporated into the reliability calculations.

The treatment of structural uncertainties is based on Taylor's expansion of expressions for failure probability, conditioned on these variables. Analytical and numerical schemes have been developed for computing the gradients in the Taylor series expansions. The analytical approach leads to exact estimates for the gradients but is difficult to implement. On the other hand, the numerical approach is more generally applicable. Here, the Taylor's expansion is carried out in the standard normal space after suitable transformations. This has the following advantages: (a) the proposed method requires fewer gradient calculations for identical orders of expansion, and (b) the computation of higher-order moments of the associated random variables are exact. Analytical and computational methods for implementing the proposed procedure have been illustrated with reference to three examples. The accuracy of the solutions obtained has been assessed by using limited amount of Monte Carlo simulations. It is found that the neglect of structural uncertainties could lead to overestimation of structural reliability, especially when excitation intensity is moderate to low. The numerical studies conducted reveal that a solution scheme that retain three terms in Taylor's expansion, provides acceptable solutions.

In the context of earthquake engineering applications, it has been illustrated that the proposed method can be used in conjunction with probabilistic seismic hazard analysis to conduct probabilistic safety assessment studies. The structural analysis has been carried out by incorporating the finite-element method with random vibration principles and theories of extremes of random processes. This reduces the dependency of the analyses on ad hoc assumptions, such as, linear structure behavior and independence between various failure modes.

Limitations of the proposed method include the inaccuracies inherited from the assumptions made in developing approximations for the extreme value distributions. These include the assumption that the level crossings for Gaussian/non-Gaussian random processes can be modelled as Poisson point processes. The assumption of the out crossings being Poisson distributed have been proved to be mathematically valid for Gaussian processes when the threshold approaches infinity [55,56]. For threshold levels of practical interest this assumption results in errors whose size and effect depends on the bandwidth of the processes [57]. However, it can be heuristically argued that for high thresholds, the out-crossings of Gaussian/non-Gaussian processes can be viewed to be statistically independent and hence can be modelled as Poisson point processes. The proposed framework is expected to inherit inaccuracies due to this assumption. An additional limitation, with reference to non-Gaussian processes, lies in the assumption that the process and its time derivative are conditionally independent. Notwithstanding these limitations, recent studies [28,30], show that the approximations lead to fairly accurate reliability estimates. Difficulties arising due to the computational intensiveness of the proposed framework can be easily handled with the cheap availability of fast computers in recent times. Moreover, unlike Monte Carlo simulations, the computational effort does not increase for reliability estimation of highly reliable structures.

Acknowledgments

The work reported in this paper forms a part of research project entitled "Seismic probabilistic safety assessment of nuclear power plant structures", funded by the Board of Research in Nuclear Sciences, Department of Atomic Energy, Government of India.

References

[1] Joint Committee on Structural Safety, Probabilistic Model Code, http://www.jcss.ethz.ch/Home/RechteSeite.html.
[2] H.O. Madsen, S. Krenk, N.C. Lind, *Methods of Structural Safety*, Prentice-Hall, Englewood Cliffs, NJ, 1986.
[3] R.E. Melchers, *Structural Reliability and Analysis and Prediction*, Wiley, Chichester, 1999.

[4] S.O. Rice, A mathematical analysis of noise, in: N. Wax (Ed.), *Selected Papers in Random Noise and Stochastic Processes*, Dover Publications, New York, 1956, pp. 133–294.
[5] Y.K. Lin, *Probabilistic Theory of Structural Dynamics*, McGraw-Hill, New York, 1967.
[6] N.C. Nigam, *Introduction to Random Vibrations*, MIT Press, Massachusetts, 1983.
[7] L.D. Lutes, S. Sarkani, *Random Vibrations: Analysis of Structural and Mechanical Vibrations*, Elsevier, Oxford, 2004.
[8] K. Breitung, R. Rackwitz, Nonlinear combination of load processes, *Journal of Structural Mechanics* 10 (2) (1982) 145–166.
[9] H.Y. Pearce, Y.K. Wen, On linearization points for nonlinear combination of stochastic load processes, *Structural Safety* 2 (1985) 169–176.
[10] Y.K. Wen, *Structural Load Modeling and Combination for Performance and Safety Evaluation*, Elsevier, Amsterdam, 1990.
[11] M. Grigoriu, Crossings on non-Gaussian translation processes, *Journal of Engineering Mechanics, ASCE* 110 (4) (1984) 610–620.
[12] M.D. Pandey, S.T. Ariaratnam, Crossing rate analysis of non-Gaussian response of linear systems, *Journal of Engineering Mechanics, ASCE* 122 (6) (1996) 507–511.
[13] H.O. Madsen, Extreme value statistics for nonlinear load combination, *Journal of Engineering Mechanics, ASCE* 111 (1985) 1121–1129.
[14] R.N. Iyengar, Estimation of yield damage in plates and shells during random vibration, *Journal of Aeronautical Society of India* 36 (1) (1984) 1–6.
[15] A. Naess, Crossing rate statistics of quadratic transformations of Gaussian processes, *Probabilistic Engineering Mechanics* 16 (2001) 209–217.
[16] A. Naess, H.C. Karlsen, Numerical calculation of the level crossing rate of second order stochastic Volterra systems, *Probabilistic Engineering Mechanics* 19 (1) (2004) 155–160.
[17] S. McWilliam, Joint statistics of combined first and second order random processes, *Probabilistic Engineering Mechanics* 19 (1) (2004) 145–154.
[18] S. Gupta, C.S. Manohar, Probability distribution of extremes of Von Mises stress in randomly vibrating structures, *Journal of Vibrations and Acoustics, ASME* 127 (6) (2005) 547–555.
[19] S. Gupta, C.S. Manohar, Improved response surface method for time variant reliability analysis of nonlinear random structures under nonstationary excitations, *Nonlinear Dynamics* 36 (2004) 267–280.
[20] A. Naess, A study of linear combination of load effects, *Journal of Sound and Vibrations* 129 (2) (1989) 83–98.
[21] D. Veneziano, M. Grigoriu, C.A. Cornell, Vector process models for system reliability, *Journal of Engineering Mechanics* 103 (EM3) (1977) 441–460.
[22] O. Ditlevsen, First outcrossing probability bounds, *Journal of Engineering Mechanics* 110 (2) (1984) 282–292.
[23] Y.K. Wen, H.C. Chen, System reliability under time varying loads: I, *Journal of Engineering Mechanics* 115 (4) (1989) 808–823.
[24] O. Hagen, L. Tvedt, Vector process out-crossings parallel system sensitivity measure, *Journal of Engineering Mechanics* 117 (10) (1991) 2201–2220.
[25] O. Hagen, Conditional and joint failure surface crossing of stochastic processes, *Journal of Engineering Mechanics* 118 (9) (1992) 1814–1839.
[26] B.J. Leira, Multivariate distributions of maxima and extremes for Gaussian vector processes, *Structural Safety* 14 (1994) 247–265.
[27] B.J. Leira, Extremes of Gaussian and non-Gaussian vector processes: a geometric approach, *Structural Safety* 25 (2003) 401–422.
[28] S. Gupta, C.S. Manohar, Development of multivariate extreme value distributions in random vibration applications, *Journal of Engineering Mechanics, ASCE* 131 (7) (2005) 712–720.
[29] C.S. Manohar, R. Ghanem, Multivariate probability distribution of ordered peaks of vector Gaussian random processes, *Probabilistic Engineering Mechanics* 20 (1) (2005) 87–96.
[30] S. Gupta, P. van Gelder, Extreme value distributions for nonlinear transformations of vector Gaussian processes, *Probabilistic Engineering Mechanics*, under review.
[31] A. Der Kiuregian, Measures of structural safety under imperfect states of knowledge, *Journal of Engineering Mechanics, ASCE* 115 (5) (1989) 1119–1140.
[32] C.S. Manohar, R.A. Ibrahim, Progress in structural dynamics with stochastic parameter variations 1987–1998, *Applied Mechanics Reviews, ASME* 52 (5) (1999) 177–197.
[33] H.M. Hwang, Seismic probabilistic risk assessment and seismic margins studies for nuclear power plants, *Probabilistic Engineering Mechanics* 3 (4) (1988) 170–178.
[34] A. Der Kiureghian, Seismic fragility assessment of structural systems towards a synthesis approach, SMiRT 15, South Korea, 1997, pp. 175–190.
[35] ASCE 4-98, Seismic analysis of safety-related nuclear structures and commentary, ISBN 078440433X, *American Society of Civil Engineers*, 1998.
[36] R.H. Chreng, Y.K. Wen, Reliability of uncertain nonlinear trusses under random excitation: I, *Journal of Engineering Mechanics, ASCE* 120 (4) (1994) 733–747.
[37] Y. Zhang, A. Der Kiureghian, First-excursion probability of uncertain structures, *Probabilistic Engineering Mechanics* 9 (1994) 135–143.
[38] C.E. Brenner, C.G. Bucher, A contribution to the SFE-based reliability assessment of nonlinear structures under dynamic loading, *Probabilistic Engineering Mechanics* 10 (1995) 265–273.
[39] S. Mahadevan, S. Mehta, Dynamic reliability of large frames, *Computers and Structures* 47 (1) (1993) 57–67.
[40] S. Gupta, C.S. Manohar, Dynamic stiffness method for circular stochastic Timoshenko beams: response variability and reliability analysis, *Journal of Sound and Vibrations* 253 (5) (2002) 1051–1085.

[41] N.L. Johnson, S. Kotz, *Discrete Distributions*, Wiley, New York, 1969.
[42] S. Coles, *An Introduction to Statistical Modeling of Extreme Values*, Springer, Berlin, 2001.
[43] A. Der Kiureghian, P.L. Liu, Structural reliability under incomplete probability information, *Journal of Engineering Mechanics, ASCE* 112 (1) (1986) 85–104.
[44] R. Courant, *Differential and Integral Calculus*, Blackie and Son Limited, London, 1934.
[45] S.K. Lele, Compact finite difference schemes with spectral like resolution, *Journal of Computational Physics* 103 (1992) 16–42.
[46] T.J. Chung, *Computational Fluid Dynamics*, Cambridge University Press, Cambridge, 2002.
[47] J.H. Ferziger, M. Peric, *Computational Methods for Fluid Dynamics*, Springer, Berlin, 2002.
[48] C.G. Bucher, U. Bourgund, A fast and efficient response surface approach for structural reliability problems, *Structural Safety* 7 (1990) 57–66.
[49] M.R. Rajashekhar, B.R. Ellingwood, A new look at the response surface approach for reliability analysis, *Structural Safety* 12 (1993) 205–220.
[50] X.L. Guan, R.E. Melchers, Effect of response surface parameter variation on structural reliability estimation, *Structural Safety* 23 (4) (2001) 429–444.
[51] S. Gupta, C.S. Manohar, An improved response surface method for the determination of failure probability and importance measures, *Structural Safety* 26 (2004) 123–139.
[52] N.A. Abrahamson, F.S. Schneider, C. Stepp, Spatial coherency of shear waves from Lotung, Taiwan large scale seismic test, *Structural Safety* 10 (1991) 145–162.
[53] ASME Boiler and Pressure Vessel Code, Division I, Appendix N12332.
[54] C.A. Cornell, Bounds on the reliability of structural systems, *Journal of Structural Division, ASCE* 93 (ST1) (1967) 171–200.
[55] H. Cramer, On the intersections between the trajectories of a normal stationary stochastic process and a high level, *Arkive Mathematics* 6 (1966) 337–349.
[56] M.R. Leadbetter, G. Lindgren, H. Rootzen, *Extremes and Related Properties of Random Sequences and Processes*, Springer, Berlin, 1983.
[57] E. Vanmarcke, On the distribution of first passage time for normal stationary random processes, *Journal of Applied Mechanics, ASME* 42 (1975) 215–220.